1984

Thermodynamics of formation of intermediate phases in the yttrium-iron and yttrium-cobalt systems

P. Ramanathan Subramanian
Iowa State University

Subramanian, P. Ramanathan

THERMODYNAMICS OF FORMATION OF INTERMEDIATE PHASES IN THE YTTRIUM-IRON AND YTTRIUM-COBALT SYSTEMS

Iowa State University PH.D. 1984

Thermodynamics of formation of intermediate phases in the yttrium-iron and yttrium-cobalt systems

by

P. Ramanathan Subramanian

A Dissertation Submitted to the
Graduate Faculty in Partial Fulfillment of the
Requirements for the Degree of
DOCTOR OF PHILOSOPHY

Department: Materials Science and Engineering
Major: Metallurgy

Approved:

Signature was redacted for privacy.

In Charge of Major Work

Signature was redacted for privacy.

For the Major Department

Signature was redacted for privacy.

For the Graduate College

Iowa State University
Ames, Iowa

1984

TABLE OF CONTENTS

GENERAL INTRODUCTION

The purpose of this investigation was to determine the Gibbs free energies, enthalpies, and entropies of formation of intermediate phases in the yttrium-iron and yttrium-cobalt systems.

Investigation of the literature showed very little experimental thermodynamic data for yttrium-transition metal alloys. Miedema (1) has developed a theoretical scheme for predicting the enthalpy of formation of binary intermetallic compounds on the basis of an atomic model. Watson and Bennett (2,3) have employed a d-electron energy band theory model to estimate the enthalpy of formation of equiatomic transition metal alloys. Detailed description of the two models will be found later. In the case of the Y-Fe and Y-Co systems, the initial values predicted by the two models were quite different. These binary systems were, therefore, chosen for the present investigation in order to provide experimental data for testing the two models.

The thermodynamics of formation of the Y-Fe and Y-Co intermediate phases were determined by the electromotive force technique. Single crystalline CaF_2 was used as the solid electrolyte and the EMF measurements were made with all components in the solid state. This technique has been used successfully by Skelton and co-workers (4-6) in the thermodynamic investigation of thorium alloy systems, and the relative simplicity of this technique makes this method the most expedient one for determining the thermodynamics of formation of Y-Fe and Y-Co intermediate phases.

Electromotive Force Cells

The basic details of the electromotive force apparatus have been described in detail by Skelton and co-workers (4). The EMF cells used in this investigation were of the type

$$Y,\ YF_3|CaF_2|YF_3,\ M,\ YM_c \qquad (1a)$$

or

$$Y,\ YF_3|CaF_2|YF_3,\ YM_a,\ YM_b \qquad (1b)$$

where M = Fe or Co, and M and YM_c or YM_a and YM_b are neighboring phases in the equilibrium diagram.

According to Darken and Gurry (7), the electrical work done on a galvanic cell operating at a potential E for a period of time such that n gram-electrons of current flow is given by

$$W_e = n E \qquad (2)$$

where F is the Faraday constant and is the charge of 1 gram-electron. Under reversible conditions, the Gibbs free energy change at constant temperature and pressure is defined by the equation

$$\Delta G = -W_e \quad . \qquad (3)$$

The free energy change for the cell reaction is, therefore, related to the EMF of the cell by the following equation:

$$\Delta G = -nFE \quad . \tag{4}$$

For an electrolyte which conducts by both electronic and ionic transfer, Steele (8) has derived the following equation for the open circuit cell voltage:

$$E_{oc} = \frac{1}{zF} \int_{\mu'_{ion}}^{\mu''_{ion}} t_{ion} \, d\mu_{ion} \tag{5}$$

where the μ's refer to the chemical potentials of the anion at the two electrodes, z is the valence, and t_{ion} is the transference number of the anion. For reversible cell operation, the solid electrolyte must exhibit only ionic conductivity. Ure (9) has found that the transference number of the fluorine ions in CaF_2 is virtually unity over the temperature range 600° to 1000°C. Hinze and Patterson (10) have shown that CaF_2 can be employed successfully as a solid electrolyte, with negligible electronic conductivity, over a wide range of temperatures and fluorine activities. Under these conditions, Eq. (5) can be written as

$$E_{oc} = \frac{1}{F} \left[\mu''_F - \mu'_F\right] = \frac{RT}{F} \ln \left[\frac{a''_{F^-}}{a'_{F^-}} \right] \tag{6}$$

where μ_F's and a_F's are the chemical potentials and activities, respectively, of fluorine in the two electrodes.

The galvanic cells in Eqs. (1a) and (1b) operate on the basis of two half-cell reactions, each corresponding to a reaction at the electrolyte-electrode interface. The half-cell reactions can be written as

$$Y + 3F^- \rightarrow YF_3 + 3e^- \tag{7}$$

and

$$3e^- + YF_3 + cM \rightarrow YM_c + 3F^- \tag{8a}$$

or

$$3e^- + YF_3 + \left(\frac{b}{a-b}\right) YM_a \rightarrow \left(\frac{a}{a-b}\right) YM_b + 3F^- \tag{8b}$$

resulting in the cell reactions

$$Y + cM \underset{\leftarrow}{\rightarrow} YM_c \tag{9a}$$

and

$$Y + \left(\frac{b}{a-b}\right) YM_a \underset{\leftarrow}{\rightarrow} \left(\frac{a}{a-b}\right) YM_b \quad . \tag{9b}$$

Under equilibrium conditions, the free energy change for the reaction in Eq. (7) is given by

$$\Delta G[7] = 0 = \Delta G^\circ[YF_3] + RT \ln \frac{a_{YF_3}(a'_{e^-})^3}{a_Y(a'_{F^-})^3} \qquad (10)$$

and the free energy change corresponding to the reaction in Eq. (8a) is

$$\Delta G[8a] = 0 = \Delta G^\circ[YM_c] - \Delta G^\circ[YF_3] + RT \ln \frac{a_{YM_c}(a''_{F^-})^3}{(a_M)^c a_{YF_3}(a''_{e^-})^3} \quad . \qquad (11)$$

Y, YM_c, and YF_3 are all solid phases with negligible mutual solubilities. Their activities can, therefore, be regarded as unity. Equations (10) and (11) can be combined to give

$$\Delta G^\circ[YM_c] = -RT \ln \frac{(a'_{e^-})^3(a''_{F^-})^3}{(a''_{e^-})^3(a'_{F^-})^3} \quad . \qquad (12)$$

The activities of the mobile electrons on each side of the cell are the same. Equations (12) and (6) can, therefore, be combined to give

$$\Delta G^\circ[YM_c] = -3FE_{oc} \qquad (13)$$

where $\Delta G^\circ[YM_c]$ is the standard free energy of formation of YM_c. If the standard free energy values are linearly dependent on the temperatures, the entropy of the cell reaction is related to the experimental EMFs by the relation

$$\Delta S^\circ = 3F\left(\frac{\partial E_{oc}}{\partial T}\right)_p \quad . \tag{14}$$

The enthalpy of formation is determined by combining the free energy values and the entropy values, and is given by

$$\Delta H^\circ = -3F\left[E_{oc} - T\left(\frac{\partial E_{oc}}{\partial T}\right)_p\right] \quad . \tag{15}$$

The relations derived above are applicable only when the galvanic cells are operated under reversible conditions.

Oriani (11) has established experimental criteria for reversibility. In a cell operating reversibly, the measured voltage should be independent of time at constant temperature, should be reproducible irrespective of whether it is approached from higher or lower temperature, and should recover its value after the passage of a small amount of current in either direction through the cell.

If the electrochemical cells are operated reversibly at fixed temperature, electromotive force values provide direct measures of the Gibbs free energies of cell reactions. Moreover, if pure solid phases

are chosen as standard states, and if the phases have invariant activities, the electromotive force data are directly convertible to standard Gibbs free energies of phase formation.

Explanation of the Format

The first section of this thesis contains a report on the thermodynamics of formation of all four intermediate phases in the Y-Fe system. This report was accepted for publication in CALPHAD journal.

The second section deals with the thermodynamics of formation of nine intermediate phases in the Y-Co system. This report has been submitted to METALLURGICAL TRANSACTIONS for publication.

THEORY

Watson-Bennett Model

Watson and Bennett (2,3) have employed an electron band theory model for predicting the enthalpy of formation of transition metal alloys at the equiatomic composition. The concept was developed by Friedel (12), who showed that the cohesion of a transition metal is partly due to the broadening of the partially filled d electron levels into a band. The Friedel model assumed a rectangular d-band density of states, for which the gain in bonding energy is given by the difference between the band center, C, and the energy of the occupied levels, E_F. This implies that filling of energy levels below the band center involves a gain in bonding energy, whereas there is a net loss of energy for electrons filling antibonding levels above the band center. According to Friedel, the cohesive energy contribution is given by

$$E_{Fr} = \int_0^{E_F} (E - C)N(E)dE \qquad (16)$$

where E_F is the Fermi level, N(E) is the density of states, and C is the band center of gravity. For rectangular density of states, Eq. (16) reduces to

$$E_{Fr} = -n_d \frac{(10 - n_d)}{20} W \qquad (17)$$

where W is the band width and n_d is the number of electrons per atom occupying the d bands.

The single particle contribution to the total d electron energy is given by

$$E = n_d C - n_d \frac{(10 - n_d)}{20} W \quad . \tag{18}$$

The enthalpy of formation of an equiatomic AB alloy is, therefore, given by the following relation:

$$\begin{aligned} \Delta E &= E_{AB} - \tfrac{1}{2}(E_A + E_B) \\ &= n_{AB}C_{AB} - n_{AB}\frac{(10 - n_{AB})}{20} W_{AB} \\ &\quad - \tfrac{1}{2}\left(n_A C_A - n_A \frac{(10-n_A)}{20} W_A + n_B C_B - n_B \frac{(10-n_B)}{20} W_B\right) \end{aligned} \tag{19}$$

where n_A, n_B, and n_{AB} are the numbers of occupied d-band levels in metals A and B and in the alloy AB, respectively, and C and W are their centers of gravity and bandwidths, respectively. In the above formulation, the elemental band centers and bandwidths are taken to be the values for the pure metals, and for a first approximation

$$n_{AB} = \frac{n_A + n_B}{2} \tag{20a}$$

and

$$C_{AB} = \frac{C_A + C_B}{2} \quad . \tag{20b}$$

The alloy bandwidth, W_{AB}, is dependent on the elemental bandwidths, W_A and W_B, and the separation, ΔC, of the two centers of gravity. From Pettifor's (13) theory

$$W_{AB} = \left[\left(\frac{W_A + W_B}{2} \right)^2 + 3(\Delta C)^2 \right]^{1/2} \tag{21}$$

where $\Delta C = C_B - C_A$.

As a result of alloying, however, the values for the band centers, C_A and C_B, and the bandwidths, W_A and W_B, corresponding to the atoms A and B in the alloy may not be the same as the values in the pure metals. A number of factors influence this shift from elemental values. Firstly, there is a volume contraction upon alloying, the molecular volume of the alloy being less than the sum of the elemental volumes. This volume contraction affects the elemental band centers of gravity and bandwidths (14). The energy change associated with the volume contraction is evaluated from bulk compressibility data.

Secondly, there is a d-electron transfer upon alloying. In order to predict the correct direction and magnitude of charge transfer, Watson and Bennett (15) have assumed that the elemental constituents in the alloy interact only with like atoms. The d-electrons are then transferred from one set of sites to the other in order to bring their local chemical potentials, E_F, to a common value, resulting in the shifting of their centers of gravity with respect to one another. Besides the shift in the band centers, there is an energy associated with the bringing of the local chemical potentials to a common value (15).

In addition, there is a d-charge transfer when the occupied d-levels of the two sites hybridize to form the alloy band. Finally, the d-electron effects are screened by interatomic conduction electron transfer. Because of the screening by the conduction electrons, the energy associated with d-electron transfer arising from hybridization can be neglected.

Therefore, the elemental band centers and bandwidths in Eq. (19) should be replaced by C_A^i and C_B^i, and W_A^i and W_B^i, respectively, with the latter values being evaluated after taking into account the changes due to volume contraction as well as the chemical potential shift. The alloy band center of gravity and bandwidth given by Eqs. (20b) and (21), respectively, are modified in a similar manner.

Therefore, the enthalpy of alloy formation can be derived as the sum of the modified version of Eq. (19), the energy associated with volume contraction, and the energy of the chemical potential shift.

Miedema Model

In this model, the Wigner-Seitz concept of atomic cells of the pure metals has been applied to the formation of a binary alloy (16). The model assumes that the volume of the atomic cells of the two types of metal atoms in a binary alloy are essentially similar, in a first-order approximation, to that for the pure elements, i.e., there is no change in atomic volumes upon alloying. The alloying energy effects, therefore, are a result of the change in the boundary conditions upon transfer of atoms from the pure metals to the alloy.

The change in boundary conditions results in two opposing effects. Firstly, there is a discontinuity in the density of electrons, n_{ws}, at boundaries between dissimilar atomic cells in the alloy. The electron density must be continuous across the boundary between dissimilar atoms. The density discontinuity, therefore, has to be removed, and this leads to a positive contribution to the alloying energy.

Secondly, the chemical potential for electrons, ϕ^*, in the two types of cells are generally different. The need for equality of the chemical potential for electrons in the alloy, therefore, results in a net charge transfer. This displacement of charge lowers the energy of the alloy and, thus, provides a negative contribution to the energy of alloying.

These two opposing effects can be combined to give the following empirical expression for the heat of formation of a binary alloy:

$$\Delta H = -P(\Delta\phi^*)^2 + Q(\Delta n_{ws}^{1/3})^2 - R \qquad (22)$$

where ΔH is the enthalpy of formation per gram atom of alloy, and P and Q are constants for a given group of alloy systems, $\Delta\phi^*$ is the difference in chemical potential for electrons in the two pure metals, and Δn_{ws} is the discontinuity in the density of electrons at the boundary between dissimilar Wigner-Seitz cells. R represents an additional energy contribution for binary alloys containing at least one transition metal, and arises from hybridization effects that occur when a metal atom with d-type electron levels comes close to a metal atom with p-type electron states. R is taken to be zero for nontransition metal alloys.

For a more quantitative description of the enthalpy of formation, ΔH, its concentration dependence has to be taken into account. The concentration dependence of ΔH involves the determination of the relative contact surface area between the atomic cells of the two dissimilar metals, A and B.

The surface area concentration of metal A, C_A^S, is given by the relation

$$C_A^S = \frac{X_A V_A^{2/3}}{X_A V_A^{2/3} + (1 - X_A) V_B^{2/3}} \qquad (23)$$

where X_A is the atomic concentration of A, and V_A and V_B are the molar volumes of the pure metals A and B, respectively.

In the model, the heat of formation is proportional to the degree, f_B^A, by which atoms of A are surrounded by neighboring B atoms. For a statistical distribution of atoms, this is given by

$$f_B^A = 1 - C_A^S \quad . \tag{24}$$

For ordered compounds in binary systems, however, the contacts between dissimilar atoms occur more frequently than for a statistical distribution. Miedema and de Châtel (16) obtained the following empirical relation for f_B^A:

$$f_B^A = (1 - C_A^S)\{1 + 8(C_A^S)^2(1 - C_A^S)^2\} \quad . \tag{25}$$

In the above equation, C_A^S is the surface area concentration of metal A, and is given by the relation in Eq. (23). As a result of alloying, however, there will be changes in atomic volumes due to charge transfer. Therefore, V_A should be replaced by $V_A(\text{alloy})$, the volume of A in the alloy. $V_A(\text{alloy})$ can be calculated from the relation

$$V_A^{2/3}(\text{alloy}) = V_A^{2/3}(\text{pure})\{1 + f \cdot f_B^A(\Delta\phi^*)\} \tag{26}$$

where f is a proportionality constant and is equal to 0.14, 0.10, 0.07, and 0.04 for monovalent, divalent, trivalent, and higher valent metals, respectively.

The heat of formation is assumed to be linearly proportional to f_B^A, and is given by the relation:

$$\Delta H_f = X_A f_B^A \Delta H_{sol}^{A \text{ in } B} \tag{27}$$

where $\Delta H_{sol}^{A \text{ in } B}$ is the heat of solution of A in B. Miedema and de Châtel (16) have shown that $\Delta H_{sol}^{A \text{ in } B}$ can be obtained from the following expression:

$$\Delta H_{sol}^{A \text{ in } B} = \frac{2 V_A^{2/3}}{((n_{ws}^A)^{-1/3} + (n_{ws}^B)^{-1/3})} [-P(\Delta\phi^*)^2 + Q(\Delta n_{ws}^{1/3})^2 - R] \quad . \tag{28}$$

Miedema (17) has shown that, for transition metals as well as nontransition metals, the density of electrons at the cell boundary, n_{ws}, can be approximately correlated with the square root of the ratio of the bulk modulus, B, and the molar volume, V_m. Values for ϕ^* have been derived from experimental data on the work function of the pure metal (17).

The enthalpy of formation of binary alloy systems of A and B can, therefore, be evaluated from the expression:

$$\Delta H_f = \frac{2 X_A f_B^A V_A^{2/3}}{((n_{ws}^A)^{-1/3} + (n_{ws}^B)^{-1/3})} [-P(\Delta\phi^*)^2 + Q(\Delta n_{ws}^{1/3})^2 - R] \quad . \tag{29}$$

In the above formulation, the parameters P and Q are empirical in nature, and are derived from experimental data on a number of alloys.

SECTION I. THERMODYNAMICS OF FORMATION OF YTTRIUM-IRON ALLOYS

ABSTRACT

Solid electrolyte electromotive force cells have been used to determine the Gibbs free energies, enthalpies and entropies of phase formation for Y_2Fe_{17}, Y_6Fe_{23}, YFe_3, and YFe_2 over the temperature range 893 K to 1271 K. Solid CaF_2 was employed as the electrolyte. The enthalpies of formation of the Y-Fe phases lie between -6 to -9 kJ/gm-atom. Comparison of the experimental values for the Gibbs energies of formation of the Y-Fe phases at 973 K with those of the Th-Fe, Th-Co, Th-Ni, La-Co and La-Ni systems show an empirical correlation with the total number of bonding electrons in these alloy systems.

INTRODUCTION

An initial review of the phase relationships in the Y-Fe system was done in 1961 by Gschneidner (1), and a second review was done in 1982 by Kubaschewski (2). Both reviews agree in acceptance of the basic diagram proposed by Domagala et al. (3). Kubaschewski, has, however, made minor revisions to phase stoichiometries to bring the diagram into accord with results from more recent crystallographic studies. The Kubaschewski version of the diagram is shown in Fig. 1. Neither Gschneidner or Kubaschewski accepted the equilibrium existence of a phase at a stoichiometry of YFe_5 that was reported by Farkas and Bauer (4) and by Nassau et al. (5). The reasons for rejection appear sound, and Taylor and Poldy (6) have been unable to find the phase. Further, it may be noted that the alloying behavior of yttrium generally parallels that of the heavier lanthanons, and the binary systems Gd-Fe (7), Tb-Fe (8), Dy-Fe (9), Ho-Fe (10-12), Er-Fe (13,14), Tm-Fe (15), and Lu-Fe (15) each have the same intermediate phases as in Fig. 1 without existence of any $LnFe_5$.

A crystallographic study by Zarechnyuk and Kripyakevich (16) found the most iron-rich phase in the Y-Fe system to have an ideal stoichiometry of Y_2Fe_{17} with a Th_2Ni_{17}-type structure. A subsequent study by Buschow (17) found the phase to be dimorphic with the higher temperature form being Th_2Ni_{17}-type and the lower temperature form being the Th_2Zn_{17}-type, but no transformation temperature has been established. Kripyakevich et al. (18) and Kharchenko et al. (19) have independently

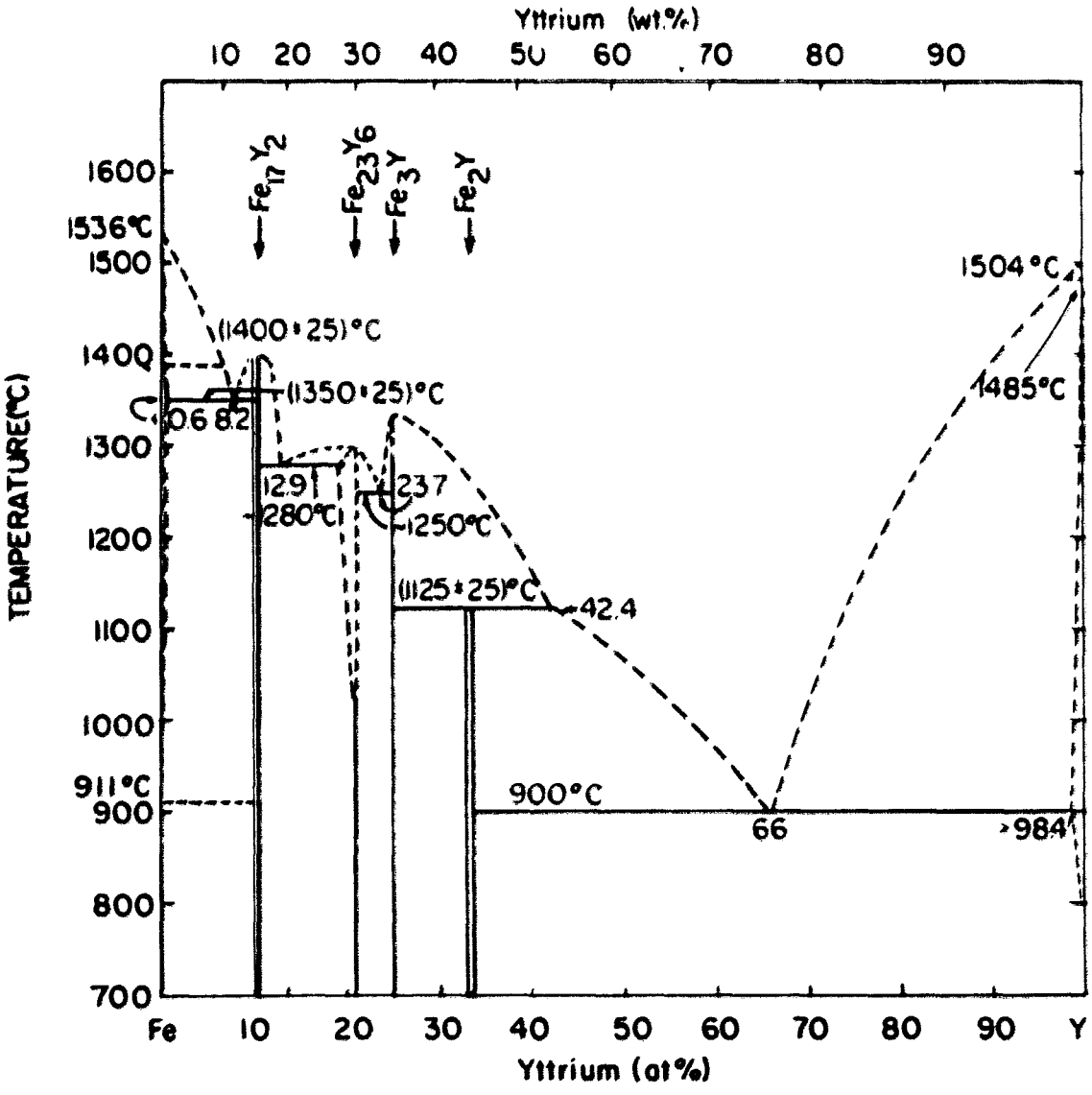

Figure 1. The yttrium-iron phase diagram

reported 'YFe_4' to have an ideal stoichiometry of Y_6Fe_{23} and to be isomorphous with Th_6Mn_{23}. Both van Vucht (20) and Buschow (21) have confirmed the existence of a phase with stoichiometry YFe_3 and with the $PuNi_3$-type structure. The most yttrium-rich phase is YFe_2 and is a Laves phase with the $MgCu_2$-type structure (5,22,23). All of these phases are structurally related and form primarily because of packing considerations.

No experimental thermodynamic data for the Y-Fe system are available. van Mal et al. (24) have estimated the heats of formation for the four intermediate phases on the basis of Miedema's theory (25), and Watson and Bennett (26-28) have developed a simple electron band theory model for predicting the order of magnitude of the heats of formation of alloys between metals with d and/or f bands. For the Y-Fe, Y-Co and Y-Ni systems, the predictions of the two theories were initially quite different, so these systems were chosen for the present EMF investigation in order to distinguish the relative validity of the two approaches. A secondary reason for the study was to develop a thermodynamic base to determine whether the competitive phase equilibria could be analyzed to explain the glass-forming tendencies (29,30) in these systems.

PROCEDURE AND RESULTS

Alloys were prepared by arc melting 6.5, 13.6, 21.2 and 29.5 at.% Y (10, 20, 30 and 40 wt.% Y) on a water-cooled copper hearth under an atmosphere of purified argon. Arc-melted buttons were inverted and remelted at least five times to ensure homogeneity. Yttrium was prepared at this laboratory and the impurity analysis for the yttrium of the latter three alloys is shown in Table 1; the yttrium in the yttrium-poor alloy with 6.5 at.% Y was slightly less pure but the dilution factor was greater so the total impurity content of the alloy was comparable. Electrolytic iron was obtained from the Glidden Company and the iron analysis is shown in Table 2. The 6.5 at.% Y alloy lay in the two-phase field between Fe and Y_2Fe_{17}, the 13.6 at.% Y alloy between Y_2Fe_{17} and Y_6Fe_{23}, the 21.2 at.% Y alloy between Y_6Fe_{23} and YFe_3, and the 29.5 at.% Y alloy between YFe_3 and YFe_2.

Fine particles of the four alloys and of yttrium were produced in a dry box under purified helium either by crushing in a diamond mortar or by filing with a tungsten carbide file. Only those particles passing through a 60 mesh screen were retained. The equilibrium phases in the 6.5, 13.6, and 21.2 at.% Y alloys are all congruently melting, so the temperatures of the EMF measurements were considered as providing adequate anneals. The YFe_2 phase of the 29.5 at.% alloy, however, decomposes by peritectic reaction, and this latter alloy was annealed for 25 days at a temperature 50° below the peritectic temperature to facilitate equilibration. For all alloys x-ray powder diffraction data were taken

Table 1. Impurity analysis of yttrium[a]

Impurity	Impurity content (at. ppm)			
	Spark Source Mass Spectrometric Analysis	Vacuum Fusion Analysis	Carbon Combustion Analysis	Absorption Analysis
H		704		
B	0.07			
C			141	
N		25		
O		834		
Mg	0.1			
Al	3			
Si	3			
Cl	3			
Ca	0.1			
Ti	0.8			
Cr	0.5			
Fe				8
Ni	3			
Cu	5			
W				22
Pb	20			
La	3			
Ce	2			
Pr	4			
Gd	2.1			
Tb	4.5			

[a]Li, Be, Na, P, S, K, V, Mn, Co, Zn, Ga, Ge, As, Se, Br, Rb, Sr, Zr, Nb, Mo, Ru, Rh, Pd, Ag, Cd, In, Sn, Sb, Te, I, Cs, Ba, Hf, Ta, Re, Os, Ir, Pt, Au, Hg, Tl, Bi, Th, U, Sc, Nd, Sm, Eu, Dy, Ho, Er, Tm, Yb, and Lu were below detectable limits by spark source mass spectrometer analysis and F was below detectable limits by absorption analysis.

Table 2. Impurity analysis of iron

Impurity	Amount wt, ppm
Oxygen	107
Nitrogen	50
Carbon	89
Hydrogen	10
Tungsten	10
Copper	<8

with a Picker diffractometer and no reflections were observed that were not characteristic of one or the other of the expected phases at the specific alloy composition.

Electrode pellets were prepared by mixing ~80 wt.% metal particles with ~20 wt.% YF_3 powder. These mixtures were transferred to a press in plastic bags containing inert gas. With the press, the pellets were compacted in a tungsten carbide die to 23,000 psi. The electrode pellets were then transferred, again under protective atmosphere, to a furnace where they were arranged to form galvanic cells, were encased in a protective boron nitride casing, and were loaded into the furnace. Single crystals of solid CaF_2 in the form of thin wafers were used as the solid electrolytes, and Y, YF_3 pellets were used as reference electrodes. Electrical contact to the electrodes was via platinum leads through tantalum discs. Cell temperatures were measured with chromel-alumel thermocouples, and EMFs were measured with a Fluke 8800A digital multimeter. The electrochemical cells were operated under purified argon atmospheres, and the cells were allowed to equilibrate for 5-6 days at elevated temperature prior to EMF measurements.

EMF measurements were made on the following galvanic cells where the electrodes on the right correspond to the four alloy compositions in the order of increasing yttrium concentration

$$Y,\ YF_3 \| CaF_2 \| YF_3,\ Fe,\ Y_2Fe_{17} \qquad (1)$$

$$Y,\ YF_3 \| CaF_2 \| YF_3,\ Y_2Fe_{17},\ Y_6Fe_{23} \qquad (2)$$

$$Y,\ YF_3 \| CaF_2 \| YF_3,\ Y_6Fe_{23},\ YFe_3 \qquad (3)$$

$$Y,\ YF_3 \| CaF_2 \| YF_3,\ YFe_3,\ YFe_2 \qquad (4)$$

and the cell reactions may be represented as

$$Y + (17/2)\ Fe \rightleftharpoons (1/2)\ Y_2Fe_{17}$$

or

$$Y + \left(\frac{b}{a-b}\right) YFe_a \rightleftharpoons \left(\frac{a}{a-b}\right) YFe_b$$

In his review of electrochemical techniques, Oriani (31) has summarized the requisite criteria for reversible cell operation. The three primary criteria are that the open circuit voltage should show no significant time variation at constant temperature, should have the same value regardless of the direction of approach to the equilibrium temperature, and should recover to the same value after passage of current in either forward or reverse direction. During the present experiments, only those data which obeyed these reversibility criteria were retained.

For reversible cell operation at fixed temperature, the Gibbs free energy of reaction is expressed by the relation:

$$\Delta G_T = -3\ F\ E^\circ \qquad (5)$$

where F is the Faraday constant, E° is the open circuit EMF, and 3 is the number of electrons per ion involved in the reaction. Measurements were made over the temperature range 893 K to 1271 K where CaF_2 is known (32) to be a good ionic conductor with negligible electronic conduction. Raw data points, though taken in random order, are listed in the order of increasing temperature in Table 3, and points from independent runs at the same composition are not differentiated. Figure 2 shows the least-squares fits of the EMF data as functions of temperature. With neglect of the very limited ranges of homogeneity which are indicated in the phase diagram, the fitted data yield the following relationships for the standard Gibbs energy of formation of the four intermediate phases:

$$Y + \frac{17}{2}\,Fe \;\rightleftharpoons\; \frac{1}{2}\,Y_2Fe_{17}$$

$$\Delta G_f^\circ\,[Y_2Fe_{17}] = 2[-3\,F\,E_1^\circ]$$
$$= -121.22 + (35.98\times10^{-3})T \text{ kJ/mole of } Y_{2/19}Fe_{17/19} \qquad (6)$$

$$Y + \frac{23}{56}\,Y_2Fe_{17} \;\rightleftharpoons\; \frac{17}{56}\,Y_6Fe_{23}$$

$$\Delta G_f^\circ[Y_6Fe_{23}] = \frac{56}{17}\,[-3\,F\,E_2^\circ] + \frac{23}{17}\,\Delta G_f^\circ[Y_2Fe_{17}]$$
$$= -3F[\frac{56}{17}\,E_2^\circ + \frac{46}{17}\,E_1^\circ]$$
$$= -234.59 + (64.90\times10^{-3})T \text{ kJ/mole of } Y_{6/29}Fe_{23/29} \qquad (7)$$

$$Y + \frac{3}{5}\,Y_6Fe_{23} \;\rightleftharpoons\; \frac{23}{5}\,YFe_3$$

Table 3. Experimental EMF data at measured temperatures for various Y-Fe compositions

Composition (at.% Y)	Temp (K)	EMF (mV)	Composition (at.% Y)	Temp (K)	EMF (mV)
6.3	893	156.6		1110	21.4
	986	146.7		1112	21.2
	1046	147.4		1125	18.8
	1073	138.3		1132	18.2
	1073	140.5		1134	17.9
	1109	138.5		1135	17.4
	1186	132.1		1144	17.3
	1187	137.7		1159	17.1
	1190	139.2		1185	16.5
	1190	134.7		1209	14.4
	1192	135.1		1209	13.3
	1192	138.2		1210	14.0
				1235	13.2
13.6	1027	57.7		1238	11.5
	1066	54.6		1271	7.9
	1078	56.3		1271	7.0
	1085	55.1			
	1127	54.0	29.5	1002	26.4
	1130	55.0		1040	28.3
	1193	53.3		1047	29.8
	1196	54.8		1061	30.4
				1071	29.7
21.2	985	28.8		1075	30.7
	991	24.1		1120	31.4
	1054	20.5		1131	34.3
	1056	21.5		1135	35.1
	1059	20.6		1140	33.4
	1066	21.4		1143	34.1
	1071	18.4		1164	34.8
	1082	22.7		1166	35.9
	1091	19.0		1170	36.0
				1173	35.6

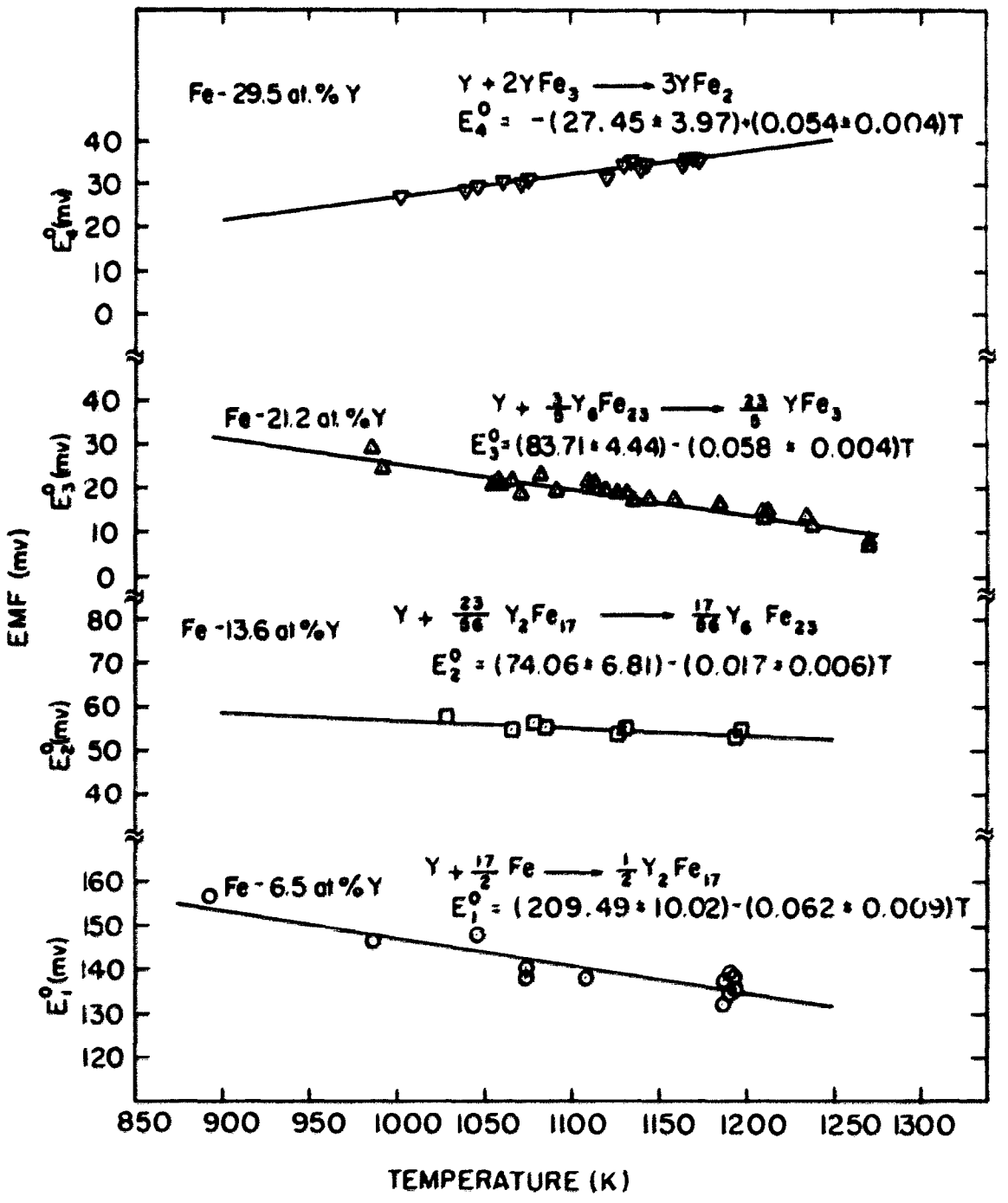

Figure 2. Electromotive force data as functions of temperature for various alloys and reactions

$$\Delta G_f^\circ[YFe_3] = \frac{5}{23}\,[-3\,F\,E_3^\circ] + \frac{3}{23}\,\Delta G_f^\circ[Y_6Fe_{23}]$$

$$= -3F[\frac{5}{23}\,E_3^\circ + \frac{168}{391}\,E_2^\circ + \frac{6}{17}\,E_1^\circ]$$

$$= -35.87 + (12.11 \times 10^{-3})T \text{ kJ/mole of } Y_{1/4}Fe_{3/4} \qquad (8)$$

$$Y + 2YFe_3 \rightleftharpoons 3YFe_2$$

$$\Delta G_f^\circ[YFe_2] = \frac{1}{3}\,[-3\,F\,E_4^\circ] + \frac{2}{3}\,\Delta G_f^\circ[YFe_3]$$

$$= -3F[\frac{1}{3}\,E_4^\circ + \frac{10}{69}\,E_3^\circ + \frac{112}{391}\,E_2^\circ + \frac{4}{17}\,E_1^\circ]$$

$$= -21.26 + (2.87 \times 10^{-3})T \text{ kJ/mole of } Y_{1/3}Fe_{2/3} \quad . \qquad (9)$$

It may be noted in Table 3 that several data points for the 6.3 at.% Y alloy are as much as 8° above the temperature of 1184 K which is the temperature of the $\alpha \rightarrow \gamma$ transformation in pure iron and which is shown in Fig. 1 by a dashed line. The dashed line, however, is most likely to be much too low for the two-phase region because data (7) which are available for Sc, Nd, and Gd show that these elements raise the temperature of the $\alpha \rightarrow \gamma$ transformation significantly and Y should therefore do likewise. On this basis no distinction has been made between the points above and below 1184 K, though it may be noted that a least-squares fit to the data with the exclusion of the higher temperature points is within the uncertainty of the fit in Fig. 2. These considerations indicate that the thermodynamic functions for intermediate phase formation in the Y-Fe system which are summarized in Table 4 may be taken as referring to pure α Fe and pure solid Y as the standard states.

DISCUSSION

The Miedema theory (33) predicts enthalpies of Y-Fe phase formation to be of the order of -2 kJ/gm-atom. In contrast, the Watson-Bennett model (28) predicts enthalpies of phase formation to be of the order of -13 kJ/gm-atom. An interpolated value of -5.3 kJ/gm-atom for an equiatomic alloy may be obtained from the data in Table 4. This number differs from both predicted values by a smaller factor of ~2 but, interestingly, in opposite sense with the Miedema value being smaller and the Watson-Bennett value being larger. Actually, as Watson and Bennett point out in their report (28), the asymmetry of the enthalpies of phase formation in this system makes the interpolated value of -5.3 kJ/gm-atom a poorer value for comparison than the more negative values of -8 to -9 kJ/gm-atom of the Y_6Fe_{23} and YFe_3 phases, so the experimental data favor the Watson-Bennett result. This single set of data for the Y-Fe system are, however, far from definitive, and additional data for the Y-Co and Y-Ni systems are being accumulated and should be useful. Preliminary data for the three Co-rich intermediate phases in the Y-Co system yield Gibbs energies of formation that are generally comparable to those of Th-Fe alloys. These Y-Co data indicate that the enthalpy of formation of an equiatomic alloy should lie in the range -12 to -26 kJ/gm-atom, but a more constrained value awaits the conclusion of experiments in progress. Current predictions for the enthalpy of formation of such an alloy are -24 kJ/gm-atom from the

Table 4. Thermodynamic functions for the formation of Y-Fe alloys[a]

Phase	$-\Delta G^{\circ}_{973}$ kJ/gm-atom	$-\Delta H^{\circ}_{973}$ kJ/gm-atom	$-\Delta S^{\circ}_{973}$ J/gm-atom K
Y_2Fe_{17}	4.54±0.05	6.38±0.31	1.90±0.28
Y_6Fe_{23}	5.91±0.07	8.09±0.49	2.24±0.44
YFe_3	6.02±0.08	8.97±0.54	3.03±0.48
YFe_2	6.15±0.09	7.09±0.61	0.96±0.55

[a]The quoted uncertainties refer to standard deviations.

Watson-Bennett approach (28) and -30 kJ/gm-atom from the Meidema approach (33).

The present values for the Gibbs energies of formation of the Y-Fe phases at 973 K are compared with those of the Th-Fe (34), Th-Co (35), Th-Ni (36), La-Co (37), and La-Ni (38) systems in Fig. 3. The Gibbs energies rather than the enthalpies were chosen for comparison because all data are based upon EMF measurements and one loses about an order of magnitude in precision when enthalpies are evaluated from the temperature dependences of the Gibbs energies. Examination of the trends in Fig. 3 shows an empirical correlation with the total number of valence electrons. This presupposes that, because the crystal structures in all systems are closely related, the number of electrons above the ion cores which are abstracted into nonbonding configurations is constant from system to system. Then, because the number of valence electrons from La and Y is three and from Th is four and because the number of electrons increment by one each from Fe to Co to Ni, the total number of bonding electrons should be greatest for the Th-Ni system and least for the Y-Fe system. Further, the number of bonding electrons should be essentially the same for La-Ni and Th-Co, and similarly, the number for La-Co should be comparable to the number for Th-Fe. Such a pattern is observable in Fig. 3. Extrapolation of this reasoning leads to the expectation that values for the Y-Co system will be found comparable to the values of the La-Co and Th-Fe systems and values for the Y-Ni system will be found comparable to the values of the La-Ni and Th-Co systems.

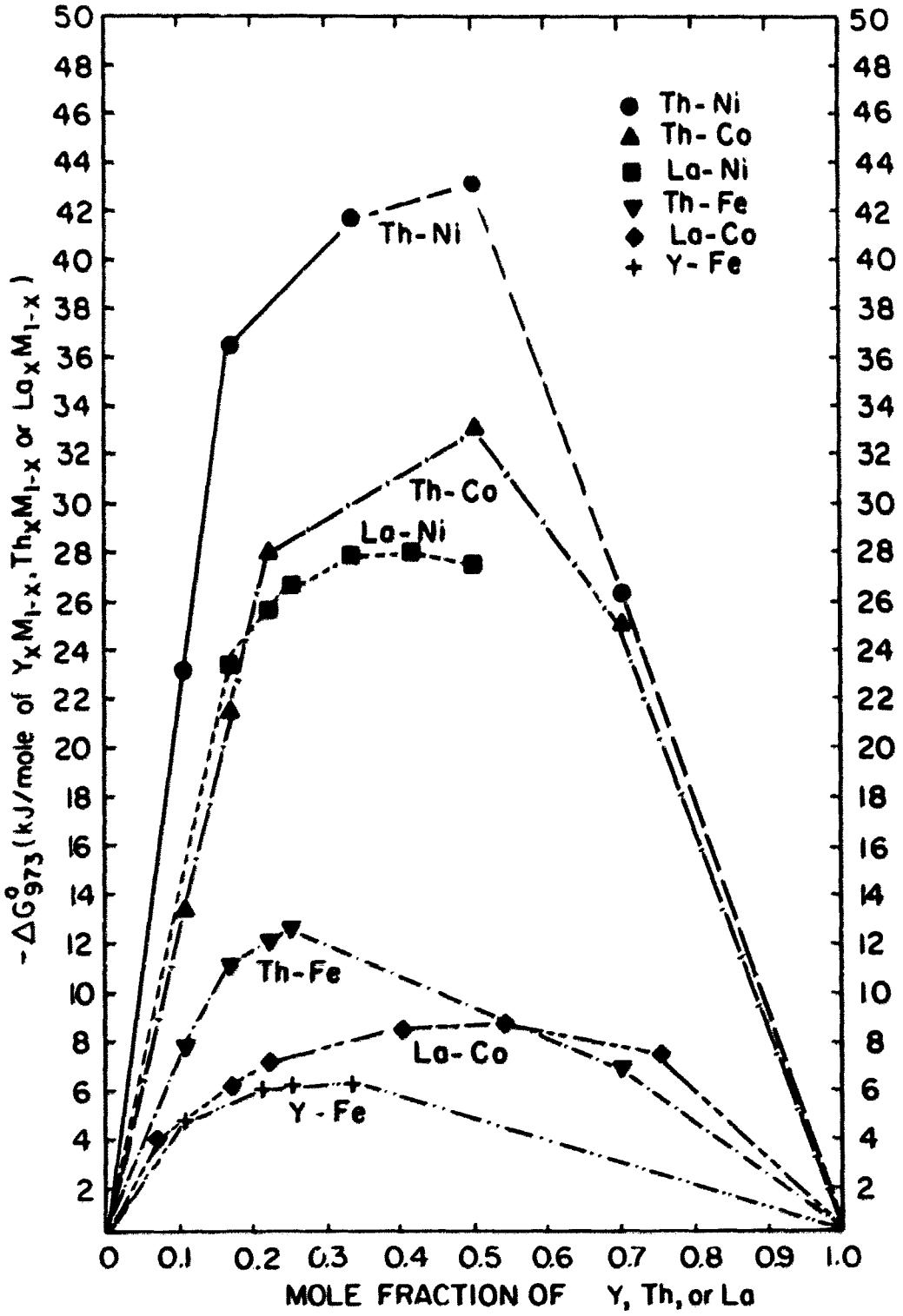

Figure 3. Comparison of experimental values for the free energies of formation of various alloys as a function of composition

REFERENCES

1. K. A. Gschneidner, "Rare Earth Alloys", Van Nostrand Co.: Princeton, New Jersey, 1961; pp. 191-193.

2. O. Kubaschewski, "IRON-Binary Phase Diagrams", Springer-Verlag: Berlin, 1982; pp. 168-170.

3. R. F. Domagala, J. J. Rausch, and D. W. Levinson, Trans. Am. Soc. Met., 1961, 53, 137-155.

4. M. S. Farkas and A. A. Bauer, U.S. AEC Report BMI-1386, 1959, 20.

5. K. Nassau, L. V. Cherry, and W. E. Wallace, J. Phys. Chem. Solids, 1960, 16, 123-130.

6. K. N. R. Taylor and C. A. Poldy, J. Less-Common Metals, 1972, 27, 255-257.

7. E. M. Savitskii, V. F. Terekhova, R. S. Torchinova, I. A. Markova, O. P. Naumkin, V. W. Koleshnichenko, and V. F. Stroganova, "Les Elements Des Terres Rares", Centre National De La Recherche Scientifique: Paris, 1970; vol. 1, pp. 47-60.

8. M. P. Dariel, J. T. Holthuis and M. R. Pickus, J. Less-Common Metals, 1976, 45, 91-101.

9. A. S. van der Goot and K. H. J. Buschow, J. Less-Common Metals, 1970, 21, 151-157.

11. T. J. O'Keefe, G. J. Roe, and W. J. James, J. Less-Common Metals, 1968, 15, 357-360.

10. T. J. O'Keefe, G. J. Roe, and W. J. James, Proceedings of the 6th Rare Earth Research Conference, Gatlinburg, Tennessee, May 3-5, 1967, pp. 449-451.

12. G. J. Roe and T. J. O'Keefe, Metall. Trans., 1970, 1, 2565-2568.

13. K. H. J. Buschow and A. S. van der Goot, Phys. Status Solidi, 1969, 35, 515-522.

14. A. Meyer, J. Less-Common Metals, 1969, 41, 41-48.

15. V. E. Kolesnichenko, V. F. Terekova, and E. M. Savitskii, In Metallovedenie Tsvetnykh Metallov I Splavov"; M. E. Drits, Ed., Izdatelistvo Nauka: Moscow, 1972; pp. 31-33.

16. O. S. Zarechnyuk, and P. I. Kripyakevich, Dopov. Akad. Nauk Ukr. RSR, 1964, 12, 1593-1595.

17. K. H. J. Buschow, J. Less-Common Metals, 1966, 11, 204-208.

18. P. I. Kripyakevich, D. P. Frankevich and Y. V. Voroshilov, Porosh. Met., 1965, 11, 55-61.

19. O. I. Kharchenko, O. I. Bodak, and E. I. Gladyshevskii, Russ. Metall. 1976, 1, 170-176.

20. J. H. N. van Vucht, J. Less-Common Metals, 1966, 10, 146-147.

21. K. H. J. Buschow, Philips Res. Rep., 1971, 26, 49-64.

22. R. J. Beaudry, J. Haefling, and A. H. Daane, Acta Cryst., 1960, 13, 743-744.

23. A. E. Dwight: Trans. Am. Soc. Met., 1961, 53, 479-500.

24. H. H. van Mal, K. H. J. Buschow, and A. R. Miedema, J. Less-Common Metals, 1976, 49, 473-475.

25. A. R. Miedema, J. Less-Common Metals, 1976, 46, 67-83.

26. R. E. Watson and L. H. Bennett, Calphad, 1981, 5, 25-40.

27. L. H. Bennett and R. E. Watson, Calphad, 1981, 5, 19-23.

28. R. E. Watson and L. H. Bennett, Calphad, 1984, in press.

29. K. H. J. Buschow and N. M. Beekmans, Solid State Commun., 1980, 35, 233-236.

30. J. J. Croat, J. Appl. Phys., 1982, 53(10), 6932-6940.

31. R. A. Oriani, J. Electrochem. Soc., 1956, 103, 194-201.

32. Y. Tretyakov and A. Kaul, In "Physics of Electrolytes"; J. Hladik, Ed., Academic Press: New York, 1972; pp. 623-677.

33. A. K. Niessen, F. R. de Boer, R. Boom, P. F. de Chatel, W. C. M. Mattens, and A. R. Miedema, Calphad, 1983, 7, 51-70.

34. W. H. Skelton, N. J. Magnani, and J. F. Smith, Metall. Trans., 1973, 4, 917-920.

35. W. H. Skelton, N. J. Magnani, and J. F. Smith, Metall. Trans., 1971, 2, 473-476.

36. W. H. Skelton, N. J. Magnani, and J. F. Smith, Metall. Trans., 1970, 1, 1833-1837.

37. T. N. Rezukhina and S. V. Kutsev, Russ. J. Phys. Chem., 1982, 56, 173-177.

38. T. N. Rezukhina and S. V. Kutsev, Russ. J. Phys. Chem., 1982, 56, 1-6.

SECTION II. THERMODYNAMICS OF FORMATION OF YTTRIUM-COBALT ALLOYS

ABSTRACT

The Gibbs free energies, enthalpies, and entropies of phase formation were determined for nine Y-Co intermediate phases from electromotive force measurements. Solid CaF_2 was employed as the electrolyte, and EMF measurements were made over the temperature range 850 K to 1200 K. The data indicate that the Gibbs free energies of formation per mole of Y reactant are nearly constant for the four Y-poor phases. Such behavior is associated with the close structural similarity of these phases. The present experimental Gibbs energy data at 973 K are compared with those of the Th-Fe, Th-Co, Th-Ni, La-Co, La-Ni, and Y-Fe systems. It was observed that the Gibbs free energy of formation can be empirically correlated with the total number of valence electrons in these alloy systems. The enthalpy of formation of an equiatomic Y-Co alloy was determined to be -27.1 kJ/mole atoms. This experimental value is in good accord with the theoretical predictions of the Miedema and Watson-Bennett models.

INTRODUCTION

Watson and Bennett (1) have suggested that the thermodynamics of phase formation for the intermediate phases in the Y-Fe, Y-Co, and Y-Ni systems should provide a good basis for evaluating the predictions of their simplified electron band theory model for estimating enthalpies of formation of binary phases that form from elements both of which utilize d-states in their bonding interactions. Pursuant to the accumulation of the desired data, EMF measurements on the Y-Fe system (2) have been completed and published. The present study is a continuation of that effort and deals with the thermodynamics of formation of the phases in the Y-Co system.

Phase diagrams for the complete Y-Co system have been proposed by Pelleg and Carlson (3) with nine intermediate phases, by Strnat et al. (4) with later minor modification by Ray (5) with eight intermediate phases, and by Buschow (6) with eight intermediate phases. These investigations agree as to the existence of phases at stoichiometries of Y_2Co_{17}, YCo_5, YCo_3, YCo_2, and Y_3Co. There now seems little doubt that a phase originally indicated by Pelleg and Carlson to be YCo_4 is actually the Y_2Co_7 phase of Strnat et al. and of Buschow. With regard to Y_2Co_7, crystallographic evidence (4,6-9) indicates the phase to be dimorphic through a transition temperature has not been established. So also is YCo_3 indicated to be dimorphic (4,6,8-12), but again no transition temperature has been established. In both instances, the polymorphic forms are simple stacking variations analogous to the stacking difference

between the cubic closest-packed and hexagonal closest-packed elemental structures. Lemaire (10,13) has discussed the structural relationships among the Co-rich Y-Co phases from Y_2Co_{17} through YCo_2; the crystal structures of these phases all result primarily from atomic packing considerations and, on this basis, the enthalpies of phase formation per mole of Y should be relatively insensitive to stoichiometry.

A phase, not found in any of the forementioned phase diagram investigations, was reported by Khan (7) as occurring at a stoichiometry of Y_5Co_{19} with a temperature range of stability at elevated temperatures. If this phase is an equilibrium phase in the pure binary system, it represents unusual behavior for Y because Y normally exhibits alloying behavior analogous to that of the heavier rare earths such as Tb, Ho, and Dy. For none of the heavier rare earths has a T_5Co_{19} phase (T representing a rare earth) been reported, though such phases occur (8) in the Co systems of the lighter rare earths: La, Ce, Pr, and Nd. In any case, the crystal structures of T_5Co_{19} phases share many of the structural features of the other Co-rich Y-Co phases. A second report (14) also indicated the Y_5Co_{19} phase to exist but found the range of stability extending to room temperature and below. These two reports of the existence of Y_5Co_{19} together with the absence of reports by other investigators who have looked in the same composition range indicate that the stability of the phase is, at best, marginal with occurrence or nonoccurrence being dependent upon minor thermodynamic contributions such as those that might arise from small variations in purity, strain, etc. On this basis, the Gibbs energy of formation of the phase, in a plot of

Gibbs energy of formation per mole of atoms vs. mole fraction of either component, should lie very near a linear interpolation between the points for the Gibbs energies of formation of YCo_5 and Y_2Co_7. Thus, even if the phase is truly a stable member of the pure binary system, the failure to observe or consider Y_5Co_{19} during the present study should introduce negligible error in the derived thermodynamic values for the other phases.

In the composition region between YCo_2 and Y_3Co, there is some disparity among the three investigations of the Y-Co phase relationships. In this composition region, Pelleg and Carlson (3) reported only Y_2Co_3, YCo, and Y_3Co_2; Strnat et al. (4) reported Y_2Co_3 and Y_3Co_2, and in a revised version of Strnat's diagram, Ray (5) reported Y_2Co_3 and Y_4Co_3; Buschow (6) found phases at 41 at.% Y and 62 at.% Y though he referred to the 62 at.% Y phase as Y_4Co_3 (57.1 at.% Y). More recently, Grover et al. (15) have examined the phase relationships in the region between 50 at.% Y and 75 at.% Y with metallography, thermal analysis, magnetic and superconductivity measurements, and x-ray diffraction. Grover et al. found the phases YCo, Y_9Co_7, Y_8Co_5, and confirmed Y_3Co. In addition, the phase Y_3Co_2, whose crystal structure was determined by Moreau et al. (16), was shown to be metastable with the phase Y_8Co_5, whose crystal structure was also determined by Moreau et al. (17), being the stable phase at 61.5 at.% Y in close accord with the composition of 62 at.% Y found by Buschow (6). A crystal structure determination by Grover et al. showed the phase, that was previously thought to be Y_4Co_3, to actually be Y_9Co_7. Indeed, the volume of the unit cell of the Y_9Co_7

structure is three times the volume of the unit cell reported by Lemaire et al. (18) for Y_4Co_3 with the Y_9Co_7 unit cell having four fewer Co atoms than three of the unit cells of the earlier proposed Y_4Co_3 structure. Actually, the structure determination by Lemaire et al. involved a number of T_4Co_3 phases with T being Y or a rare earth, and the primary structure determination was done on a single crystal of $Ho_4Co_{3.07}$ whose 43.4 at.% Co is very close to the 43.7 at.% Co of Y_9Co_7, so the possibility exists that all 'T_4Co_3' phases are T_9Co_7 phases.

Crystallographic data for the various Y-Co phases are shown in Table 1, and an eclectic phase diagram for the Y-Co system is shown in Fig. 1. In general, the peritectic and eutectic temperatures have uncertainties of the order of 10-15°. The diagram of Fig. 1 is compatible with the findings of the present investigation in that phases were observed at the stoichiometries of Y_2Co_{17}, YCo_5, Y_2Co_7, YCo_3, YCo_2, Y_2Co_3, Y_9Co_7, Y_8Co_5, and Y_3Co but not at Y_5Co_{19}, YCo, nor Y_3Co_2. The absence of YCo is discussed in more detail in the subsequent text. It should be emphasized that in the Y-Co system many phases, including glasses (19-21), are in competition for existence. The relative stabilities among these competitive phases are obviously delicate so that the appearance or nonappearance of a phase may rest upon quite minor considerations of kinetics, purity, strain, etc. It is believed that the present thermodynamic measurements represent equilibrium measurements for Y-Co alloys prepared from Y and Co of specific analyzed purity and, while other Y-Co alloys with minor differences in impurity content might differ with respect to the presence or absence of one or another phase, similar

Table 1. Crystal systems, lattice parameters, and crystal structure types reported for various Y-Co alloys

Compound	Crystal System	Structure Type	Lattice Parameters (Å)[a]	References
Y_2Co_{17}	Hexagonal	Th_2Ni_{17}	a = 8.341 c = 8.125	4,(8),10
YCo_5	Hexagonal	$CaCu_5$	a = 4.948±0.003 c = 3.975±0.002	3,4,7,8, 13,22,(23)
Y_2Co_7	Hexagonal	Ce_2Ni_7	a = 5.007 c - 24.143	4,(7)
	Rhombohedral	Gd_2Co_7	a = 5.03 c = 36.91	6,7,(8),9
YCo_3	Hexagonal	$CeNi_3$	a = 5.020±0.005 c = 24.40±0.03	4,9,10,11, (12)
	Rhombohedral	$PuNi_3$	a = 8.634±0.009 α_0 = 33.80°±0.08°	6,8,9,(12)
YCo_2	Cubic	$MgCu_2$	a = 7.216±0.002	4,10,(24)
Y_2Co_3	Cubic	Gd_2Co_3	a = 7.996	(3)
Y_4Co_3	Hexagonal	Ho_4Co_3	a = 11.529±0.004 c = 4.041±0.002	9,(18),25, 26,27,28
Y_3Co_2	Orthorhombic	Dy_3Ni_2	a = 12.248 b = 9.389 c = 3.975	(16)
Y_8Co_5	Monoclinic	Not reported	a = 7.058 b = 7.286 c = 24.277 β = 102.11°	(17)
Y_3Co	Orthorhombic	Al_3Ni	a = 7.026 b = 9.454 c = 6.290	6,(8)

[a]Lattice parameters are from the references given in parentheses.

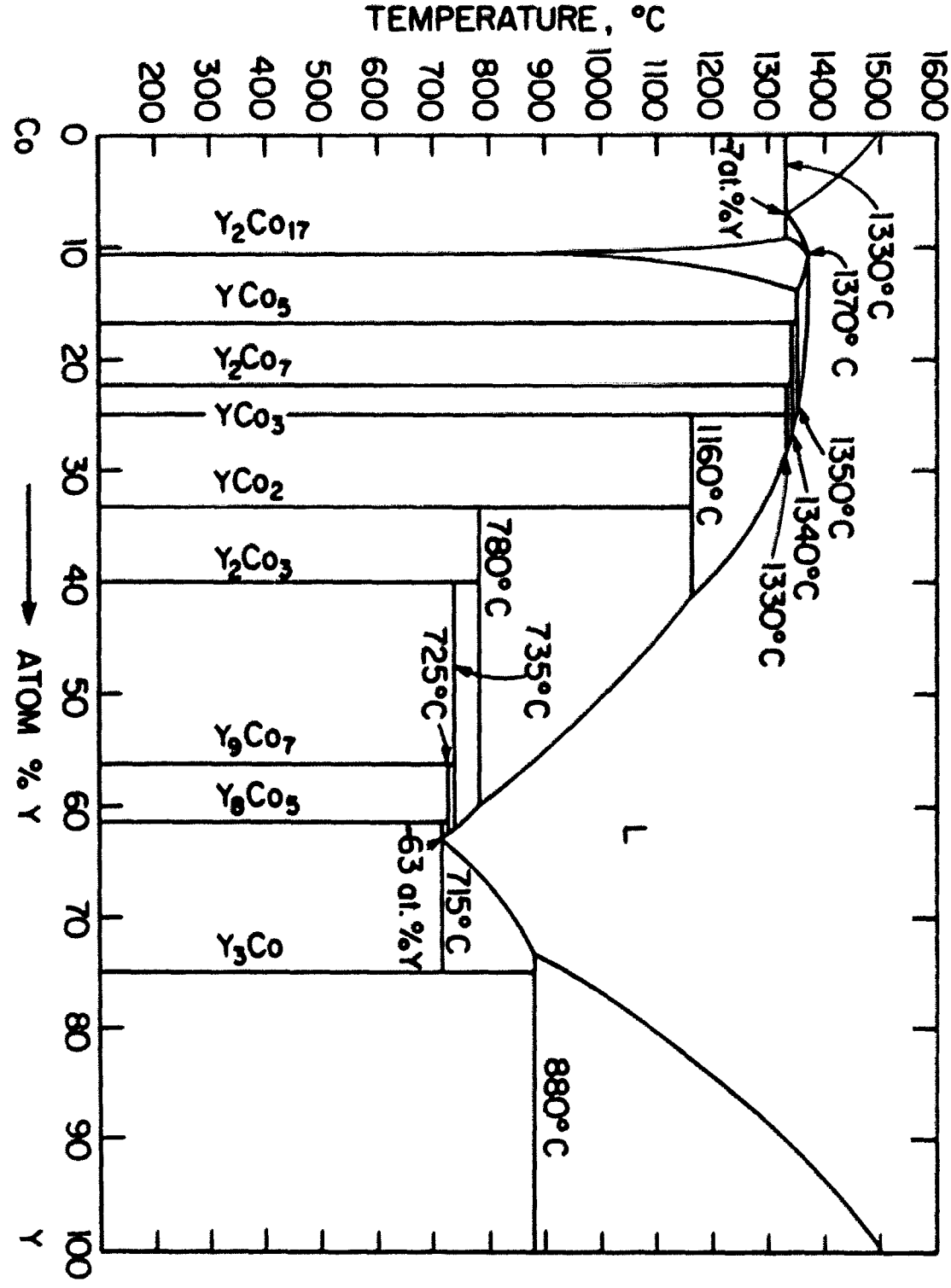

Figure 1. The yttrium-cobalt phase diagram

thermodynamic measurements on those alloys should yield thermodynamic data for equivalent phases in close accord. In essence, small differences in purity should cause small differences in enthalpies and entropies. These small differences, particularly those in entropies because of the temperature factor, modify the relative stabilities of competitive phases but make relatively little difference in the overall contour of the Gibbs energy of alloy formation as a function of composition.

EXPERIMENTAL PROCEDURE AND RESULTS

Alloys were prepared by arc melting appropriate amounts of cobalt and yttrium on a water-cooled copper hearth under an atmosphere of pure argon. Homogenization of the alloys was ensured by successively inverting and remelting the arc-melted buttons at least five times. Yttrium was prepared at this laboratory and its impurity analysis was reported in the earlier study (2). Impurity analysis of the cobalt is shown in Table 2. Six alloys were prepared in the region 6-40 at.% Y. These alloys had compositions of 6.9, 14.2, 18.1, 23.5, 30.7, and 35.2 at.% Y, and lay within the two-phase fields, respectively, between Co and Y_2Co_{17}, Y_2Co_{17} and YCo_5, YCo_5 and Y_2Co_7, Y_2Co_7 and YCo_3, YCo_3 and YCo_2, and YCo_2 and Y_2Co_3. In the region 40-80 at.% Y, four alloys were prepared with compositions 44.8, 55.2, 58.2, and 66.5 at.% Y. The former two alloys lie on either side of the equiatomic composition, and were prepared in order to verify or refute the presence of the YCo phase. The 58.2 at.% Y and 66.5 at.% Y were located in the two-phase field between Y_9Co_7 and Y_8Co_5 and between Y_8Co_5 and Y_3Co, respectively.

Alloys that formed through peritectic reactions were sealed in tantalum crucibles and annealed for 25-30 days at a temperature ~25° below the peritectic temperature to ensure the formation of equilibrium phases. The 6.9 at.% Y and 66.5 at.% Y alloys passed through eutectic transformations and were not heat treated.

Fine particles were produced from the brittle alloys by crushing in a diamond mortar, and from nonbrittle alloys and yttrium by filing with

Table 2. Impurity analysis of cobalt[a]

Impurity	Amount (at. ppm)	Impurity	Amount (at. ppm)
Li	0.1	Ti	10
B	0.1	Cr	0.6
C	9	Mn	1.2
N	10	Fe	100
O	17	Ni	320
F	0.9	Cu	27
Na	9	Zn	75
Mg	2	Se	3
Al	2	Sr	3
Si	80	I	0.4
Cl	3	Ba	2
K	10	Hg	0.21
Ca	10	Dy	1.8

[a]Impurities were analyzed by spark source mass spectrometry. Be, P, S, Sc, V, Ga, Ge, As, Br, Rb, Y, Zr, Nb, Mo, Ru, Rh, Pd, Ag, Cd, In, Sn, Sb, Te, Cs, Jf, Ta, W, Re, Os, Ir, Pt, Au, Tl, Pb, Bi, Ra, Th, U, La, Ce, Pr, Nd, Sm, Eu, Gd, Tb, Ho, Ir, Tm, Yb, and Lu were below detectable limits by spark source mass spectrometric analysis.

a tungsten carbide file. Large particles were removed by passing the powders through a 60-mesh copper sieve. All operations for the preparation of the powders were performed in a dry box under purified helium.

For x-ray verification of the phases present in each alloy, fine metal particles were sealed into capillary glass tubes inside the dry box. For the 6.9, 14.2, 18.1, 23.5, 30.7, 35.2, 58.2, and 66.5 at.% Y alloys, Debye-Scherrer powder diffraction data showed reflections characteristic of the two equilibrium phases to be expected for the specific alloy composition on the basis of the phase relationships in Fig. 1. Diffraction patterns from the 44.8 and 55.2 at.% Y alloys showed identical diffraction maxima with regard to line position but with some intensity differences. This indicates the absence of a phase at a stoichiometry of YCo. Both these alloys, therefore, lie in the same two-phase field between Y_2Co_3 and Y_9Co_7. Linear analyses of photomicrographs from both alloys showed the percentage of each of the constituent phases to be in accord with phase compositions of Y_2Co_3 and Y_9Co_7 in corroboration of the x-ray evidence for the absence of YCo. Metallographic examination of all alloys showed two-phase microstructures in amounts qualitatively in accord with the alloy composition and the phase compositions of the diagram in Fig. 1.

Electrode pellets were prepared in a dry box by mixing metal powder with ~20 wt.% YF_3 powder. The powder mixtures were transferred into tungsten carbide dies, and the dies were taken to an external press in plastic bags filled with purified helium. The mixtures were then compacted to 25,000 psi in the tungsten carbide dies. The electrode pel-

lets were arranged to form electrochemical cells inside a boron nitride cell assembly. Single crystals of CaF_2 were used as solid electrolytes and were obtained from Optovac Inc. Tungsten foils and platinum leads were used as electrical contacts in the galvanic cell. Cell voltages were monitored with a Fluke 8800A digital multimeter and temperatures were measured with a chromel-alumel thermocouple. After assembly of the cell inside a Lindberg Hevi-Duty resistance furnace, the system was flushed several times with 99.999% pure argon. The cells were then heated to 200°C, and maintained at that temperature under vacuum for several hours. The system was next filled with argon to a pressure slightly above atmospheric, and the cell temperature was raised to the desired value. Typically, a period of 5-6 days was allowed for equilibration prior to voltage measurements. In the present EMF measurements, equilibration was considered to be attained if the voltage was steady within ±1 mV over a period of four hours.

EMF measurements were made over the temperature range 850-1200 K with electrochemical cells of the type

$$Y,\ YF_3 \| CaF_2 \| YF_3,\ Co,\ Y_2Co_{17} \qquad (1)$$

or

$$Y,\ YF_3 \| CaF_2 \| YF_3,\ YCo_a,\ YCo_b \qquad (2)$$

where YCo_a and YCo_b are neighboring phases in the temperature-composition diagram. Cell reactions can be writen as

$$Y + \frac{17}{2}\,Co \;\rightleftarrows\; \frac{1}{2}\,Y_2Co_{17} \qquad (3)$$

or

$$Y + \left(\frac{b}{a-b}\right) YCo_a \;\rightleftarrows\; \left(\frac{a}{a-b}\right) YCo_b \quad . \qquad (4)$$

The criteria for reversible cell operation are that the cell voltage should be independent of time at fixed temperature, should have the same value regardless of the direction of approach to the temperature of measurement, and should recover to the same value after the passage of a small quantity of current in either direction through the cell. During the present experiments, measurements which failed to satisfy these reversibility criteria were rejected. In addition, polarization tests were conducted by shorting the electrochemical cell and tracing the recovery of the EMF to its original value within 30-45 minutes.

If the electrochemical cells are operated reversibly at fixed temperature and pressure, then the Gibbs free energy change for the cell reaction is related to the EMF of the cell by the expression (29)

$$\Delta G^\circ_T = -nFE^\circ \qquad (5)$$

where F is the Faraday constant, E° is the open circuit EMF, and n is the number of electrons involved in the cell reaction and is 3 per ion of Y in the reaction. Though taken in random order, experimental data points are listed in the order of increasing temperature in Table 3. Least-squares fits of the experimental EMF data as functions of temperature are shown both graphically and analytically in Figs. 2 and 3. For some of the cell reactions, EMF data were taken from two independent runs, and these are indicated in the figures. There are limits to the temperature range available for EMF measurements. For phases which decompose peritectically, the upper limit of the temperature range is determined by the peritectic decomposition temperature and the lower limit is set by the ionic mobility necessary for ionic conduction in the solid electrolyte. For the Y-Co alloys, the available temperature range decreases with increasing Y content; for this reason, only a limited number of data points were accumulated for alloys with the two highest Y contents.

The solid solubility of Y in Co is negligible, and there is no appreciable range of homogeneity in any of the intermediate phases at the temperature of measurement. On this basis, the pure solid phases can be chosen as standard states with invariant activities in the alloys. The present EMF data, therefore, yield standard Gibbs free energies of phase formation as follows:

Table 3. Experimental electromotive force data at measured temperatures for various Y-Co compositions

Composition (at.% Y)	Temp (K)	EMF (mV)	Composition (at.% Y)	Temp (K)	EMF (mV)
6.9	Run 1		23.5	884	239.3
	1070	253.7		890	239.7
	1071	261.4		900	238.5
	1071	258.8		979	242.1
	1079	256.3		1028	232.5
	1101	255.4		1035	237.9
	1113	259.7		1046	237.0
	1114	259.6		1049	230.9
	1120	260.6		1065	230.1
	1131	259.9		1099	232.5
	1135	262.3		1102	232.5
	1138	256.0		1107	234.8
	1140	256.4		1124	238.7
	1143	257.0			
			30.7	927	143.1
	Run 2			967	140.6
	1087	257.3		971	141.2
	1090	257.9		989	145.8
	1105	252.8		1001	143.2
	1106	253.3		1005	141.1
	1111	255.1		1022	141.1
	1116	257.6		1048	141.2
	1145	257.3		1124	236.3
	1145	255.5			
			35.2	996	80.8
14.2	973	242.9		999	77.4
	1031	239.2		1002	74.9
	1086	240.5		1005	76.6
	1147	238.9		1011	75.3
	1153	239.3		1012	75.2
	1158	238.9		1013	75.6
				1014	71.6
18.1	967	241.6		1018	74.3
	1084	235.1		1020	73.0
	1116	231.0		1024	74.3
	1134	232.5		1028	75.0
	1162	228.9		1036	69.0
	1164	231.3		1048	73.5
	1174	227.6		1049	69.8
	1202	226.1		1055	67.8
				1056	68.3

Table 3. Continued

Composition (at.% Y)	Temp (K)	EMF (mV)	Composition (at.% Y)	Temp (K)	EMF (mV)
44.8	932	54.5	58.2	Run 1	
	938	50.5		866	46.7
	941	50.7		933	55.2
	949	48.8		953	57.7
	950	49.9		987	58.5
	954	47.4			
	957	46.4		Run 2	
	970	43.9		943	48.6
				944	53.0
55.2	889	49.0		945	47.6
	899	50.1		950	50.7
	903	51.1			
	915	53.5	66.5	Run 1	
	919	51.2		958	45.7
	940	56.2		987	41.7
	948	52.8			
	952	53.9		Run 2	
	955	53.5		850	38.0
	968	52.4		860	41.8
	976	48.4			
	983	53.7			
	987	46.4			
	993	51.6			
	997	45.0			

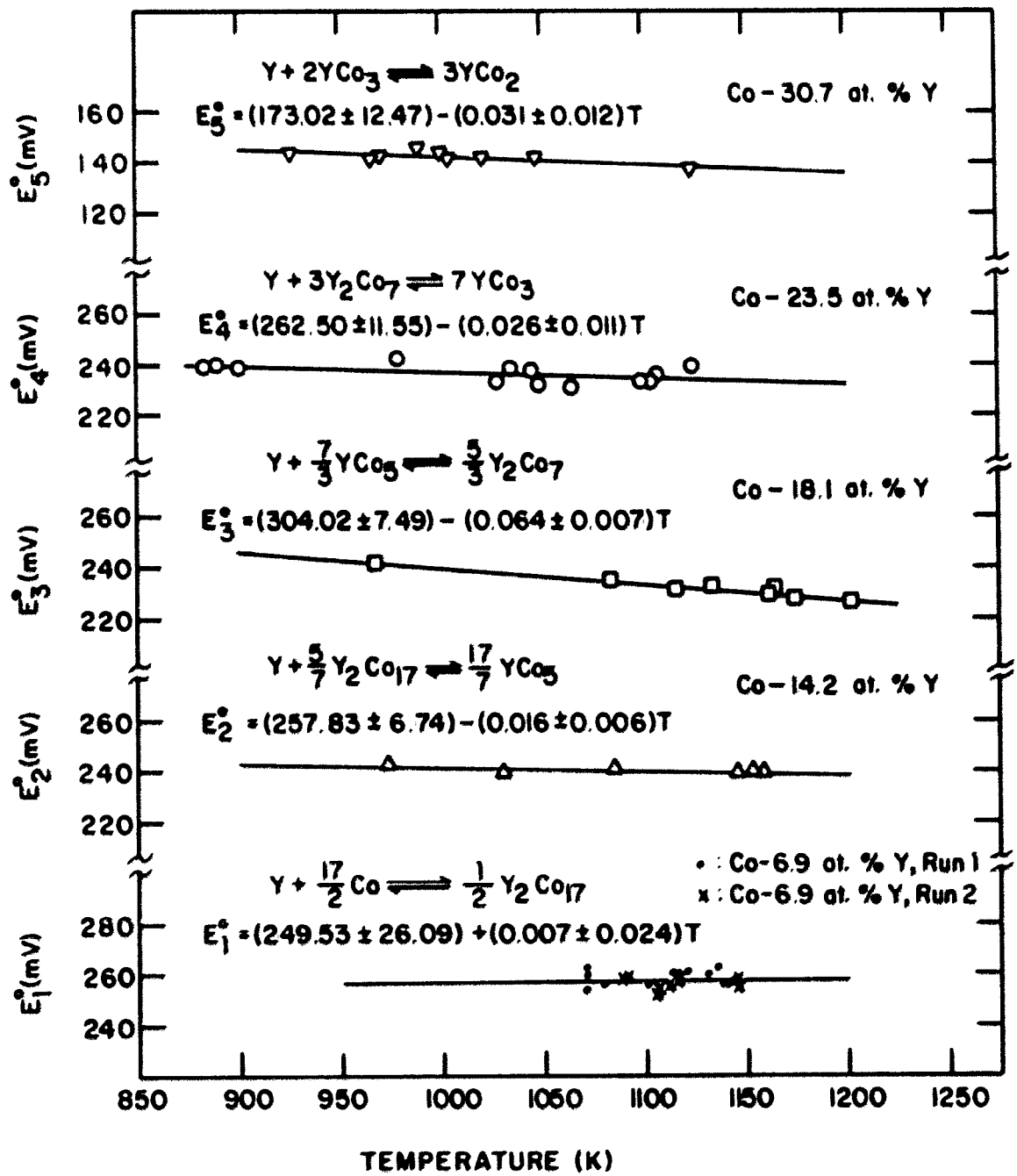

Figure 2. Electromotive force data as functions of temperature for various alloys and reactions

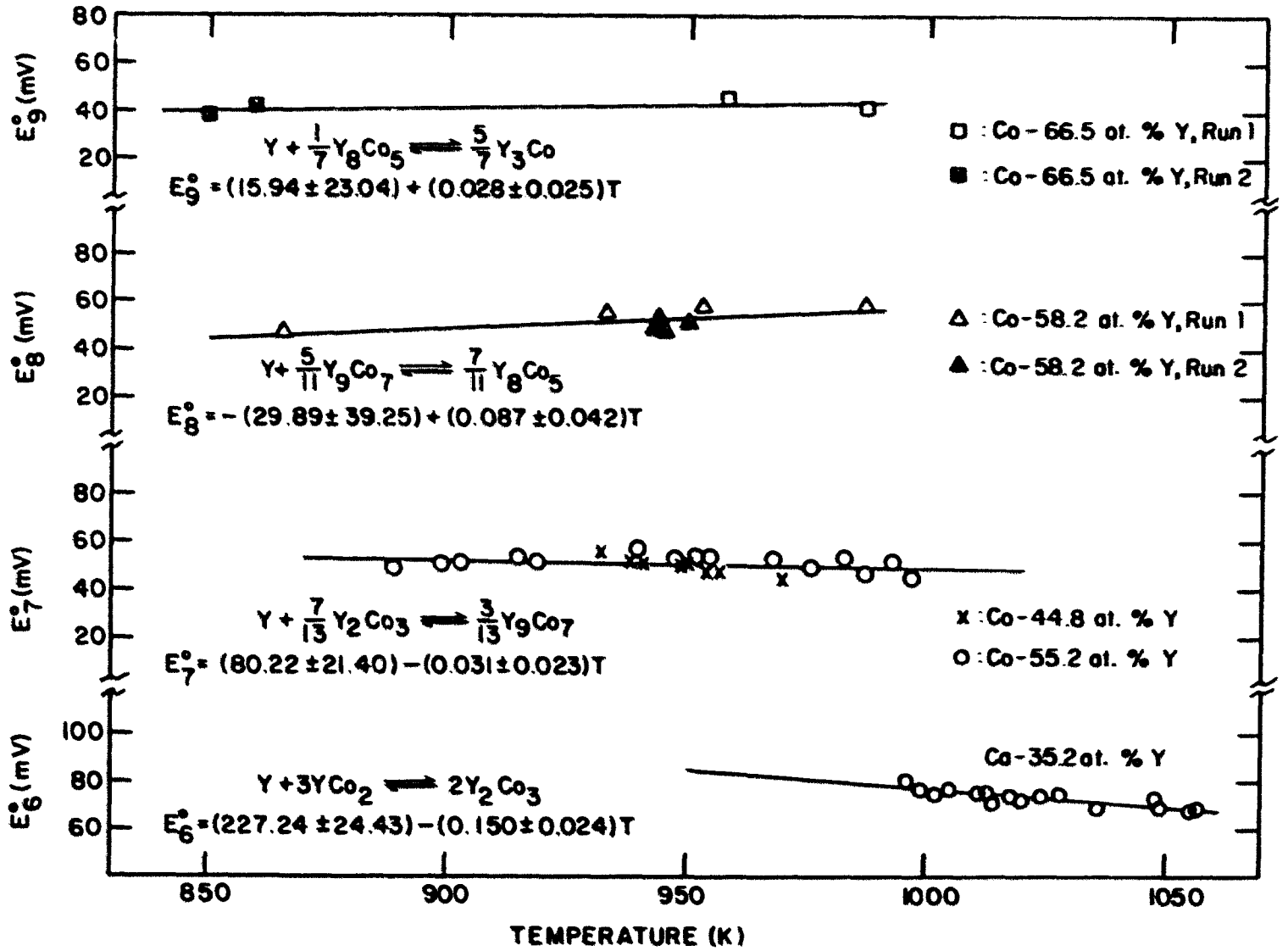

Figure 3. Electromotive force data as functions of temperature for various alloys and reactions

$$Y + \frac{17}{2}\,Co \;:\; \frac{1}{2}\,Y_2Co_{17}$$

$$\Delta G_f^\circ[Y_2Co_{17}] = 2[-3FE_1^\circ]$$

$$= -144.39 - (4.05 \times 10^{-3})T \text{ kJ/mole} \qquad (6)$$

$$Y + \frac{5}{7}\,Y_2Co_{17} \;:\; \frac{17}{7}\,YCo_5$$

$$\Delta G_f^\circ[YCo_5] = \frac{7}{17}[-3FE_2^\circ] + \frac{5}{17}\Delta G_f^\circ[Y_2Co_{17}]$$

$$= -3F\left[\frac{7}{17}E_2^\circ + \frac{10}{17}E_1^\circ\right]$$

$$= -73.18 + (0.72 \times 10^{-3})T \text{ kJ/mole} \qquad (7)$$

$$Y + \frac{7}{3}\,YCo_5 \;:\; \frac{5}{3}\,Y_2Co_7$$

$$\Delta G_f^\circ[Y_2Co_7] = \frac{3}{5}[-3FE_3^\circ] + \frac{7}{5}\Delta G_f^\circ[YCo_5]$$

$$= -3F\left[\frac{3}{5}E_3^\circ + \frac{49}{85}E_2^\circ + \frac{14}{17}E_1^\circ\right]$$

$$= -155.23 + (12.15 \times 10^{-3})T \text{ kJ/mole} \qquad (8)$$

$$Y + 3\ Y_2Co_7 \rightleftharpoons 7\ YCo_3$$

$$\Delta G_f^\circ[YCo_3] = \frac{1}{7}[-3F E_4^\circ] + \frac{3}{7}\Delta G_f^\circ[Y_2Co_7]$$

$$= -3F\left[\frac{1}{7}E_4^\circ + \frac{9}{35}E_3^\circ + \frac{21}{85}E_2^\circ + \frac{6}{17}E_1^\circ\right]$$

$$= -77.38 + (6.27 \times 10^{-3})T \text{ kJ/mole} \qquad (9)$$

$$Y + 2\ YCo_3 \rightleftharpoons 3\ YCo_2$$

$$\Delta G_f^\circ[YCo_2] = \frac{1}{3}[-3F E_5^\circ] + \frac{2}{3}\Delta G_f^\circ[YCo_3]$$

$$= -F[E_5^\circ + \frac{2}{7}E_4^\circ + \frac{18}{35}E_3^\circ + \frac{42}{85}E_2^\circ + \frac{12}{17}E_1^\circ]$$

$$= -68.27 + (7.17 \times 10^{-3})T \text{ kJ/mole} \qquad (10)$$

$$Y + 3\ YCo_2 \rightleftharpoons 2\ Y_2Co_3$$

$$\Delta G_f^\circ[Y_2Co_3] = \frac{1}{2}[-3F E_6^\circ] + \frac{3}{2}\Delta G_f^\circ[YCo_2]$$

$$= -3F\left[\frac{1}{2}E_6^\circ + \frac{1}{2}E_5^\circ + \frac{1}{7}E_4^\circ + \frac{9}{35}E_3^\circ + \frac{21}{85}E_2^\circ + \frac{6}{17}E_1^\circ\right]$$

$$= -135.28 + (32.45 \times 10^{-3})T \text{ kJ/mole} \qquad (11)$$

$$Y + \frac{7}{13} Y_2Co_3 \rightleftharpoons \frac{3}{13} Y_9Co_7$$

$$\Delta G^\circ_f[Y_9Co_7] = \frac{13}{3} [-3 F E^\circ_7] + \frac{7}{3} \Delta G^\circ_f[Y_2Co_3]$$

$$= -3F \left[\frac{13}{3} E^\circ_7 + \frac{7}{6} E^\circ_6 + \frac{7}{6} E^\circ_5 + \frac{1}{3} E^\circ_4 + \frac{3}{5} E^\circ_3 + \frac{49}{85} E^\circ_2 + \frac{14}{17} E^\circ_1 \right]$$

$$= -416.23 + (114.58 \times 10^{-3})T \text{ kJ/mole} \qquad (12)$$

$$Y + \frac{5}{11} Y_9Co_7 \rightleftharpoons \frac{7}{11} Y_8Co_5$$

$$\Delta G^\circ_f[Y_8Co_5] = \frac{11}{7} [-3 F E^\circ_8] + \frac{5}{7} \Delta G^\circ_f[Y_9Co_7]$$

$$= -3F \left[\frac{11}{7} E^\circ_8 + \frac{65}{21} E^\circ_7 + \frac{5}{6} E^\circ_6 + \frac{5}{6} E^\circ_5 + \frac{5}{21} E^\circ_4 + \frac{3}{7} E^\circ_3 \right.$$

$$\left. + \frac{7}{17} E^\circ_2 + \frac{10}{17} E^\circ_1 \right]$$

$$= -283.72 + (42.29 \times 10^{-3})T \text{ kJ/mole} \qquad (13)$$

$$Y + \frac{1}{7} Y_8Co_5 \rightleftharpoons \frac{5}{7} Y_3Co$$

$$\Delta G^\circ_f[Y_3Co] = \frac{7}{5} [-3 F E^\circ_9] + \frac{1}{5} \Delta G^\circ_f[Y_8Co_5]$$

$$= -3F\left[\frac{7}{5}E^{\circ}_{9} + \frac{11}{35}E^{\circ}_{8} + \frac{13}{21}E^{\circ}_{7} + \frac{1}{6}E^{\circ}_{6} + \frac{1}{6}E^{\circ}_{5} + \frac{1}{21}E^{\circ}_{4}\right.$$

$$\left. + \frac{3}{35}E^{\circ}_{3} + \frac{7}{85}E^{\circ}_{2} + \frac{2}{17}E^{\circ}_{1}\right]$$

$$= -63.20 - (2.89 \times 10^{-3})T \text{ kJ/mole} \qquad (14)$$

Table 4 lists values for the thermodynamic functions of formation for the nine Y-Co intermediate phases. The Gibbs free energies of formation have been calculated for 973 K, and all the tabulated values are on a per mole of atoms base.

Table 4. Thermodynamic functions for the formation of Y-Co alloys: Gibbs free energies of formation at 973 K and mean values for enthalpies and entropies of formation in the range 850 to 1200 K[a]

Phase	$-\Delta G^{\circ}_{973}$ kJ/mol atoms	$-\Delta H^{\circ}_{850\text{-}1200}$ kJ/mol atoms	$-\Delta S^{\circ}_{850\text{-}1200}$ J/k mol atoms
Y_2Co_{17}	7.81±0.10	7.60±0.80	-0.21±0.73
YCo_5	12.08±0.11	12.20±0.87	0.15±0.80
Y_2Co_7	15.93±0.12	17.25±0.96	1.35±0.87
YCo_3	17.81±0.13	19.35±1.05	1.57±0.94
YCo_2	20.41±0.14	22.76±1.33	2.38±1.25
Y_2Co_3	20.72±0.16	27.06±1.90	6.49±1.81
Y_9Co_7	19.00±0.18	26.02±3.07	7.16±3.11
Y_8Co_5	18.63±0.23	21.83±4.07	3.25±4.21
Y_3Co	16.51±0.36	15.80±4.98	-0.72±5.27

[a]The quoted uncertainties refer to standard deviations.

DISCUSSION

The present experimental values for the Gibbs free energies of formation of the Y-Co intermediate phases at 973 K are shown graphically in Fig. 4. The Gibbs energy values for the Y-Fe (2), La-Co (30), La-Ni (31), Th-Fe (32), Th-Co (33), and Th-Ni (34) systems and partial data for the Y-Ni system (35) are also included in the figure for comparison. In an earlier study (2), it was noted that there is an empirical correlation between the Gibbs energies of formation and the total number of bonding electrons in these systems. The number of electrons occupying the 3d-levels of the transition-metal component in these intermediate phases increases by one each from Fe to Co to Ni. The valence electron contribution from Y and La is three, and from Th is four. If one assumes that the number of electrons occupying the nonbonding states is the same in all these systems, this would imply that the total number of bonding electrons is least for the Y-Fe system, about the same for the Y-Co, Th-Fe and La-Co systems, and again the same for the Y-Ni, Th-Co and La-Ni systems, and greatest for the Th-Ni system. Examination of the trends in Fig. 4 shows that, with the exception of the abnormally low values for the La-Co system, there is qualitative accord between the data and the number of valence electrons. Particularly good agreement may be noted between Y-Co and Th-Fe and between Y-Ni and Th-Co in the transition metal-rich regions.

It is seen in Fig. 4 that there is a linear relation between the Gibbs energy of formation and the Y concentration for the four Y-poor

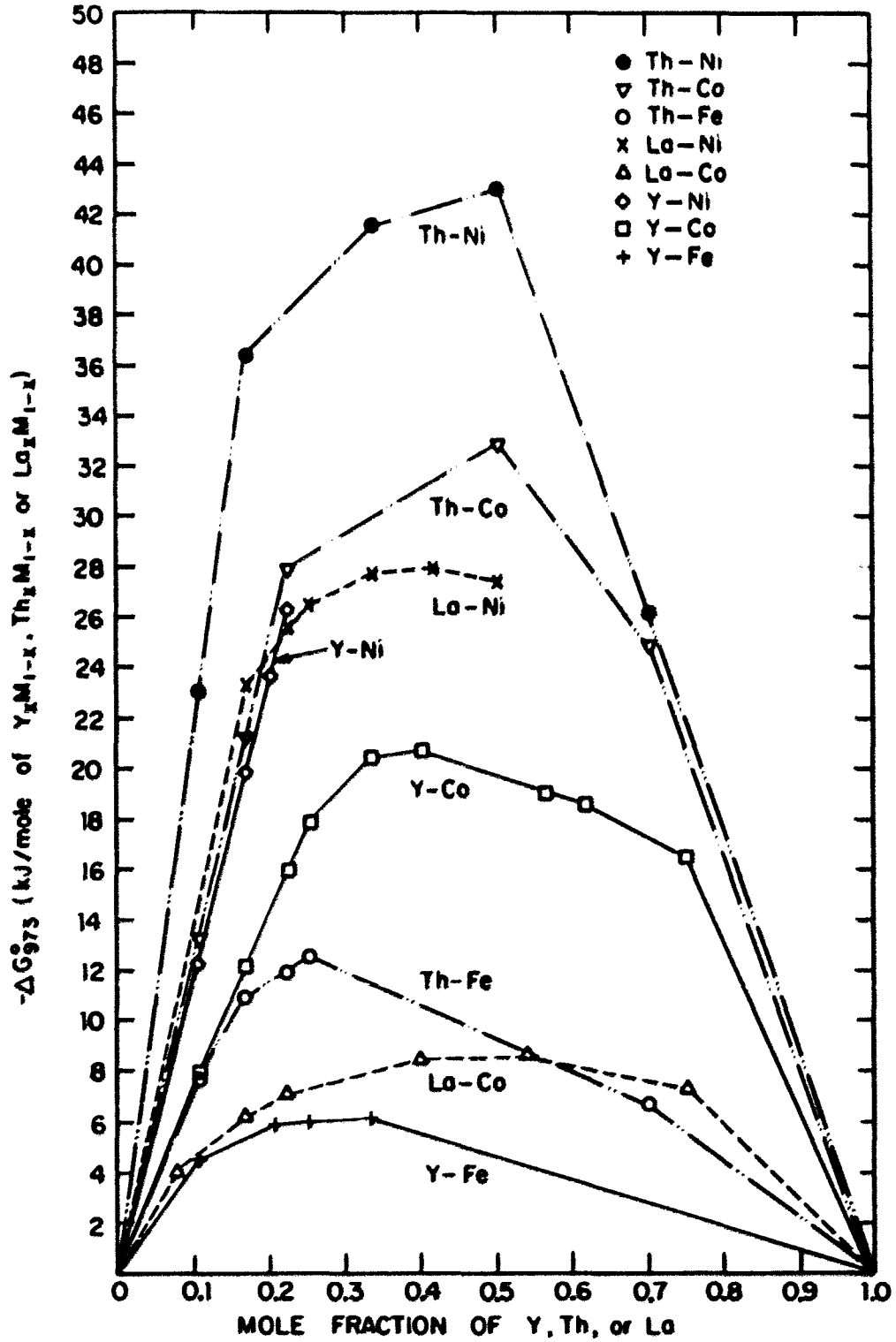

Figure 4. Comparison of experimental values for the free energies of formation of various alloys as a function of composition

phases in the Y-Co system. This implies that free energy values per mole of Y reactant are essentially constant for all these phases. Such behavior is attributable to the previously noted structural similarity of these four phases (10,13).

The present experimental values for the enthalpies of formation of the Y-Co intermediate phases are shown in Fig. 5. Niessen and co-workers (36) have computed the theoretical enthalpies of Y-Co phase formation on the basis of Miedema's theory (37). Their values are also shown in Fig. 5, along with the predicted value for YCo from the Watson-Bennett model (38). Watson and Bennett have indicated that, for systems in which the composition dependence of the enthalpy of phase formation is asymmetric, the observed maxima in the enthalpy values, rather than the interpolated value, should be compared with the estimated value for the equiatomic composition. With this approach, the experimental value for the enthalpy of formation of an equiatomic Y-Co alloy would be equal to -27.1 kJ/mole atoms. The Watson-Bennett model (38) predicts the enthalpy of formation to be -25.1 kJ/mole atoms, and the Miedema theory (36) predicts a value of -31 kJ/mole atoms. It may, therefore, be noted that the experimental value from this study lies between the two predictions and is in good agreement with both.

Table 5 shows a comparison of the theoretical predictions of the Watson-Bennett and Miedema models with the experimental enthalpies of formation for the equiatomic alloys in the Y-M, Th-M, and La-M systems (M ≡ Fe, Co, and Ni). It may be noted that the Miedema predictions are acceptable approximations to the experimental values in three out of

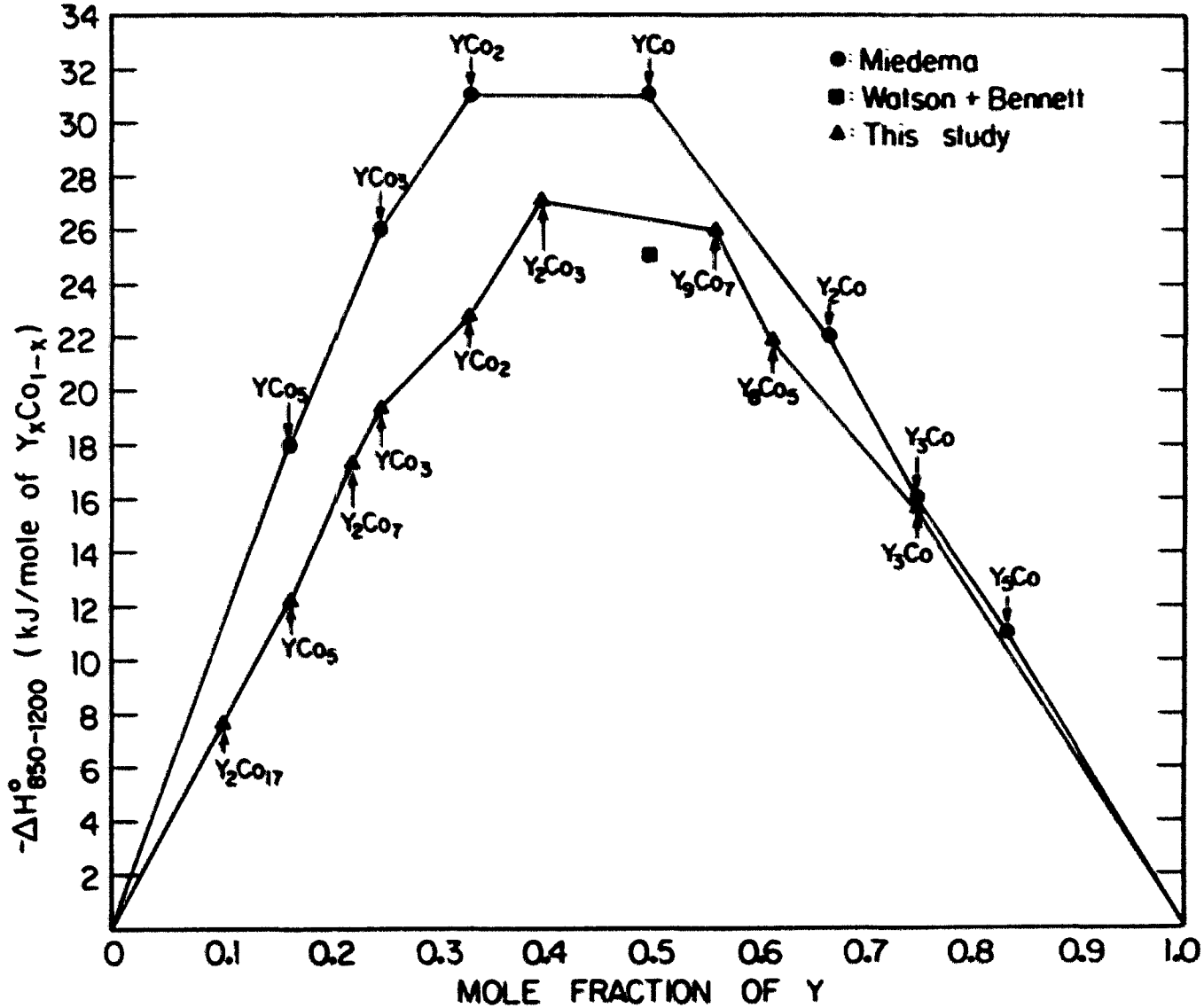
34
32
30
28
26
24
22
20
18
16
14
12
10
8
6
4
2
0
0.1
0.2
0.3
0.4
0.5
0.6
0.7
0.8
0.9
1.0
$-\Delta H^{\circ}_{850-1200}$ (kJ/mole of Y_xCo_{1-x})
MOLE FRACTION OF Y
Miedema
Watson + Bennett
This study
YCo_2
YCo
YCo_3
Y_2Co_3
Y_9Co_7
Y_2Co
YCo_5
YCo_2
Y_6Co_5
Y_3Co
YCo_3
Y_2Co_7
Y_3Co
Y_5Co
YCo_5
Y_2Co_{17}

Table 5. Comparison between theoretical predictions and experimental values for the enthalpies of formation of selected equiatomic transition metal alloys

Alloy	Watson & Bennett	Miedema	Experimental[a]	References
	$-\Delta H$(kJ/mol atoms)	$-\Delta H$(kJ/mol atoms)	$-\Delta H$(kJ/mol atoms)	
YFe	12.6	2	9	(2)
YCo	25.1	31	27.1	This study
YNi	25.1	43		
ThFe	25.1	15	24.8	(32)
ThCo	49.2	43	46.8	(33)
ThNi	53.1	54	45.3	(34)
LaFe	1.9	-6	Not available	
LaCo	5.8	24	8.6	(30)
LaNi	2.9	17	31.2	(31)

[a]Experimental data refer to the observed maximum value.

seven instances while the Watson-Bennett predictions are acceptable approximations in six out of seven instances, and, even in those cases where both predictions are acceptable, the Watson-Bennett values are slightly nearer the experimental values. EMF measurements in progress on the Y-Ni system will provide an additional experimental value for comparison with predictions, and the comparison with this value should be particularly meaningful in differentiating the predictive reliability of the two models because for the Y-Ni system the predictions differ by almost a factor of two.

REFERENCES

1. R. E. Watson, Brookhaven National Laboratory, Upton, New York, and L. H. Bennett, National Bureau of Standards, Washington, D.C., 1982, private communication.

2. P. R. Subramanian and J. F. Smith, Calphad, 1984, 8(4), 297-307.

3. J. Pelleg and O. N. Carlson, J. Less-Common Metals, 1965, 9, 281-288.

4. K. J. Strnat, W. Ostertag, N. J. Adams, and J. C. Olson, Proceedings of the 5th Rare Earth Research Conference, Ames, Iowa, 30 August - 1 September 1965, Vol. 9, pp. 281-288.

5. A. E. Ray, Cobalt, 1974, 1, 13-20.

6. K. H. J. Buschow, Philips Res. Rep., 1971, 26, 49-64.

7. Y. Khan, Phys. Status Solidi A, 1974, 23, 425-434.

8. K. H. J. Buschow, Rep. Prog. Phys., 1977, 40, 1179-1256.

9. K. H. J. Buschow, Les Eléments de Terres Rare, 1970, 1, 101-112.

10. R. Lemaire, Cobalt, 1966, 33, 201-211.

11. J. H. N. van Vucht, J. Less-Common Metals, 1965, 10, 146-147.

12. J. F. Smith and D. A. Hansen, Acta Cryst., 1965, 19, 1019-1024.

13. R. Lemaire, Cobalt, 1966, 32, 132-140.

14. I. Z. Rahman, D. Melville, and W. I. Khan, Phys. Status Solidi A, 1982, 70, K175-K179.

15. A. K. Grover, B. R. Coles, B. V. B. Sarkissian, and H. E. N. Stone, J. Less-Common Metals, 1982, 86, 29-36.

16. J. M. Moreau, E. Parthé, and D. Paccard, Acta Cryst. B, 1975, 31, 747-749.

17. J. M. Moreau, D. Paccard, and E. Parthé, Acta Cryst. B, 1976, 32, 496-500.

18. R. Lemaire, J. Schweizer, and J. Yakinthos, Acta Cryst. B, 1969, 25, 710-713.

19. S. M. Bhagat, J. N. Lloyd, and N. Heiman, J. Appl. Phys., 1978, 49(3), 1683-1685.

20. N. Heiman and N. Kazama, Phys. Rev. B, 1978, 17(5), 2215-2220.

21. D. Gignoux, D. Givord, and A. Liénard, J. Appl. Phys., 1982, 53(3), 2321-2323.

22. E. Krén, J. Schweizer, and F. Tasset, Phys. Rev., 1969, 186(2), 479-483.

23. J. Schweizer and F. Tasset, J. Phys. F, 1980, 10, 2799-2818.

24. B. J. Beaudry, J. F. Haefling, and A. H. Daane, Acta Cryst., 1960, 13, 743.

25. C. Berthet-Colominas, J. Laforest, R. Lemaire, R. Pauthenet, and J. Schweizer, Cobalt, 1968, 39, 97-101.

26. S. Wada, T. Kohara, K. Asayama, Y. Kitaoka, Y. Kohori, and N. Ishikawa, Solid State Commun., 1983, 48(1), 5-8.

27. E. Gratz, H. R. Kirchmayr, V. Sechovsky, and E. P. Wohlfarth, J. Magn. Magn. Matls., 1980, 21, 191-195.

28. K. Yvon, H. F. Braun, and E. Gratz, J. Phys. F, 1983, 13, L131-L135.

29. L. S. Darken and R. W. Gurry, "Physical Chemistry of Metals", McGraw-Hill Book Co.: New York, 1983; p. 431.

30. T. N. Rezkhina and S. V. Kutsev, Russ. J. Phys. Chem., 1982, 56, 173-177.

31. T. N. Rezukhina and S. V. Kutsev, Russ. J. Phys. Chem., 1982, 56, 1-6.

32. W. H. Skelton, N. J. Magnani, and J. F. Smith, Metall. Trans., 1973, 4, 917-920.

33. W. H. Skelton, N. J. Magnani, and J. F. Smith, Metall. Trans., 1971, 2, 473-476.

34. W. H. Skelton, N. J. Magnani, and J. F. Smith, Metall. Trans., 1970, 1, 1833-1837.

35. P. R. Subramanian and J. F. Smith, Ames Laboratory, Iowa State University, Ames, Iowa, 1984, unpublished research.

36. A. K. Niessen, F. R. de Boer, R. Boom, P. F. de Châtel, W. C. M. Mattens, and A. R. Miedema, Calphad, 1983, 7(1), 51-70.

37. A. R. Miedema, J. Less-Common Metals, 1976, 46, 67-83.

38. R. E. Watson and L. H. Bennett, Calphad, 1984, in press.

GENERAL SUMMARY

The Gibbs free energies, enthalpies, and entropies of formation have been determined for the intermediate phases in the Y-Fe and Y-Co systems. The thermodynamics of formation of the intermediate phases were measured by the electromotive force technique with single crystalline CaF_2 as the solid electrolyte. The EMF data were taken over the temperature range 800 K to 1300 K.

The enthalpy values for the Y-Fe alloys lie in the range -6 to -9 kJ/gm-atom, while the values for the Y-Co phases lie between -7 and -28 kJ/gm-atom. The experimental values have been compared with the theoretical model of Miedema and that of Watson and Bennett. For the Y-Fe system, the experimental data tends to favor the Watson-Bennett approach. In the case of the Y-Co system, however, the experimental value is in good accord with both predictions.

The Gibbs free energies of formation of the Y-Fe and Y-Co phases at 973 K were compared with those of the La-Co, La-Ni, Th-Fe, Th-Co, and Th-Ni systems, and it was observed that the free energies can be correlated with the total number of bonding electrons in these systems. Data for the Y-Co alloys indicate that the Gibbs free energies of formation per mole of yttrium reactant are nearly constant for the yttrium-poor phases. This behavior is associated with the close structural similarity of the yttrium-poor phases, and has also been observed for equivalent intermediate phases in the Th-Fe, Th-Co, and Th-Ni systems.

REFERENCES

1. A. R. Miedema, J. Less-Common Metals, 1976, 46, 67-83.

2. R. E. Watson and L. H. Bennett, Calphad, 1981, 5, 25-40.

3. L. H. Bennett and R. E. Watson, Calphad, 1981, 5, 19-23.

4. W. H. Skelton, N. J. Magnani, and J. F. Smith, Metall. Trans., 1970, 1, 1833-1837.

5. W. H. Skelton, N. J. Magnani, and J. F. Smith, Metall. Trans., 1971, 2, 473-476.

6. W. H. Skelton, N. J. Magnani, and J. F. Smith, Metall. Trans., 1973, 4, 917-920.

7. L. S. Darken and R. W. Gurry, "Physical Chemistry of Metals", McGraw-Hill Book Co.: New York, 1953; pp. 422-423.

8. B. C. H. Steele, In "Electromotive Force Measurements in High-Temperature Systems"; C. B. Alcock, Ed., American Elsevier Publishing Co.: New York, 1968; pp. 3-27.

9. R. W. Ure, Jr., J. Chem. Phys. 1957, 26, 1363-1373.

10. J. W. Hinze and J. W. Patterson, J. Electrochem. Soc., 1973, 120, 96-99.

11. R. A. Oriani, J. Electrochem. Soc., 1956, 103, 194-201.

12. J. Friedel, In "The Physics of Metals"; J. M. Ziman, Ed., Cambridge University Press: Cambridge, England, 1969; pp. 340-408.

13. D. G. Pettifor, Phys. Rev. Lett., 1979, 42, 846-850.

14. L. Hodges, R. E. Watson, and H. Ehrenreich, Phys. Rev. B, 1972, 5, 3953-3971.

15. R. E. Watson and L. H. Bennett, Phys. Rev. Lett., 1979, 43, 1130-1134.

16. A. R. Miedema and P. F. de Châtel, In "Theory of Alloy Phase Formation"; L. H. Bennett, Ed., The Metallurgical Society of AIME: Warrendale, Pennsylvania, 1980; pp. 344-389.

17. A. R. Miedema, J. Less-Common Metals, 1973, 32, 117-136.

ACKNOWLEDGEMENTS

It gives me immense pleasure to thank Dr. J. F. Smith for his guidance, enthusiasm, patience, advice, and encouragement throughout the course of this investigation. It is a privilege to have had a chance to work with him, and I will cherish it in my memory for a long time to come.

I owe special thanks to Mr. J. D. Greiner for his assistance with the EMF apparatus; and to Mr. B. J. Beaudry for his assistance in the preparation of the alloys.

I would like to extend my sincere gratitude to my parents for their constant encouragement. Last but not least, I am sincerely grateful to my wife, Annapurna, for her patience and moral support during this investigation.